Journal of Sedimentary Research

Journal of Sedimentary Research, 2006, v. 76, 364–381
Research Article
DOI: 10.2110/jsr.2006.020

CAMBRIAN DEPOSITIONAL HISTORY OF THE ZANSKAR VALLEY REGION OF THE INDIAN HIMALAYA: TECTONIC IMPLICATIONS

P.M. MYROW,[1] K.E. SNELL*,[1] N.C. HUGHES,[2] T.S. PAULSEN,[3] N.A. HEIM,[4] AND S.K. PARCHA[5]
[1]Department of Geology, Colorado College, Colorado Springs, Colorado 80903, U.S.A.
[2]Department of Earth Sciences, University of California, Riverside, California 92521, U.S.A.
[3]Department of Geology, University of Wisconsin, Oshkosh, Wisconsin 54901, U.S.A.
[4]Department of Geology, University of Georgia, Athens, Georgia 30602, U.S.A.
[5]Wadia Institute of Himalayan Geology, Dehra Dun, Uttranchal 248001, India
e-mail: pmyrow@coloradocollege.edu

ABSTRACT: **A well-preserved Cambrian section in the Zanskar Valley of northern India has previously been interpreted to record the transition from a passive to an active tectonic margin related to Cambrian–Ordovician orogenesis. This interpretation has been used to support the tectonostratigraphic interpretation of other successions across the Tethyan Himalaya. Our detailed paleoenvironmental analysis significantly revises the tectonic and depositional history of these Cambrian deposits: no definitive record of impending Cambrian–Ordovician orogenesis is recorded in these late Middle Cambrian rocks.**

A critical transition from an ~ 125-m-thick, stromatolite-bearing carbonate deposit, the Karsha Formation, into shale and sandstone of the Kurgiakh Formation, was interpreted to represent tectonically induced drowning of a carbonate platform. Siliciclastic strata of the Kurgiakh Formation were thought to record deep-water flysch deposition in a tectonically active foreland basin next to an arc-trench system. This interpretation was based on sandstone beds with classic Bouma sequences. We show that these event beds in the Kurgiakh instead contain hummocky cross-stratification, quasi-planar lamination, and combined-flow ripple stratification, all of which reflect deposition in shallow-marine, storm-influenced environments. Thus, although the Karsha carbonate platform may have been drowned, it did not culminate in deep-sea flysch deposition, and this in turn eliminates a major line of evidence linking Kurgiakh deposition to the onset of Cambrian–Ordovician orogenesis. Other aspects of Cambrian–Ordovician deposits of northern India also shed doubt on the proposed link between Kurgiakh sedimentation and the Cambrian–Ordovician orogenic event. First, our improved biostratigraphic database suggests that the transition from the Karsha carbonate to the Kurgiakh Formation may have predated the main phase of Cambrian–Ordovician orogenesis, as recorded by overlying Ordovician molasse, by as much as 20–30 My. Second, published data from the Ordovician molasse indicate northward paleocurrents, which are parallel to those recorded by siliciclastic deposits of the Parahio Formation below the Karsha, and thus are at odds with standard models of foreland basin development for the Cambrian–Ordovician event.

Our sedimentological analysis of depositional cycles of the Parahio Formation indicates that these strata record storm-influenced environments from offshore marine to shoreface to fluvial settings. This is at odds with previous paleoenvironmental interpretations that ranged from deep-sea flysch to intertidal deposits. Paleocurrent data for marine and fluvial facies of the Parahio Formation in both Zanskar and the Spiti Valley to the south indicate northeast sediment transport. This supports the view that the Parahio and overlying carbonate of the Karsha Formation record the ancient northern passive margin of India during the Cambrian and that these strata may be distal equivalents of the younger Cambrian deposits of the Lesser Himalaya.

INTRODUCTION

Tectonic models for the Himalaya attempt to explain the formation of basic lithotectonic zones in the Himalaya. Most of these have focused on the structural, igneous, and stratigraphic signature of the Cenozoic collision of India with Asia. However, an understanding of earlier depositional and tectonic events in the Himalaya, including Cambrian–Ordovician orogenesis associated with the amalgamation of Gondwanaland, may be critical for unraveling first-order stratigraphic and structural patterns in the present-day orogen (Garzanti et al. 1986; DeCelles et al. 2000; Gehrels et al. 2003; Myrow et al. 2003).

There are three current hypotheses concerning the relationship between Cambrian sedimentary successions of the Tethyan and Lesser Himalaya, two of the three northern Himalayan lithotectonic zones that are separated by high-grade metamorphic rock of the Greater Himalaya: (1) the Lesser and Tethyan Himalaya were part of a continuous passive margin (Searle 1986; Brookfield 1993; Corfield and Searle 2000); (2) the

* Present Address: Department of Earth Sciences, University of California, Santa Cruz, California 95064, U.S.A.

 1527-1404/06/076-364/$03.00

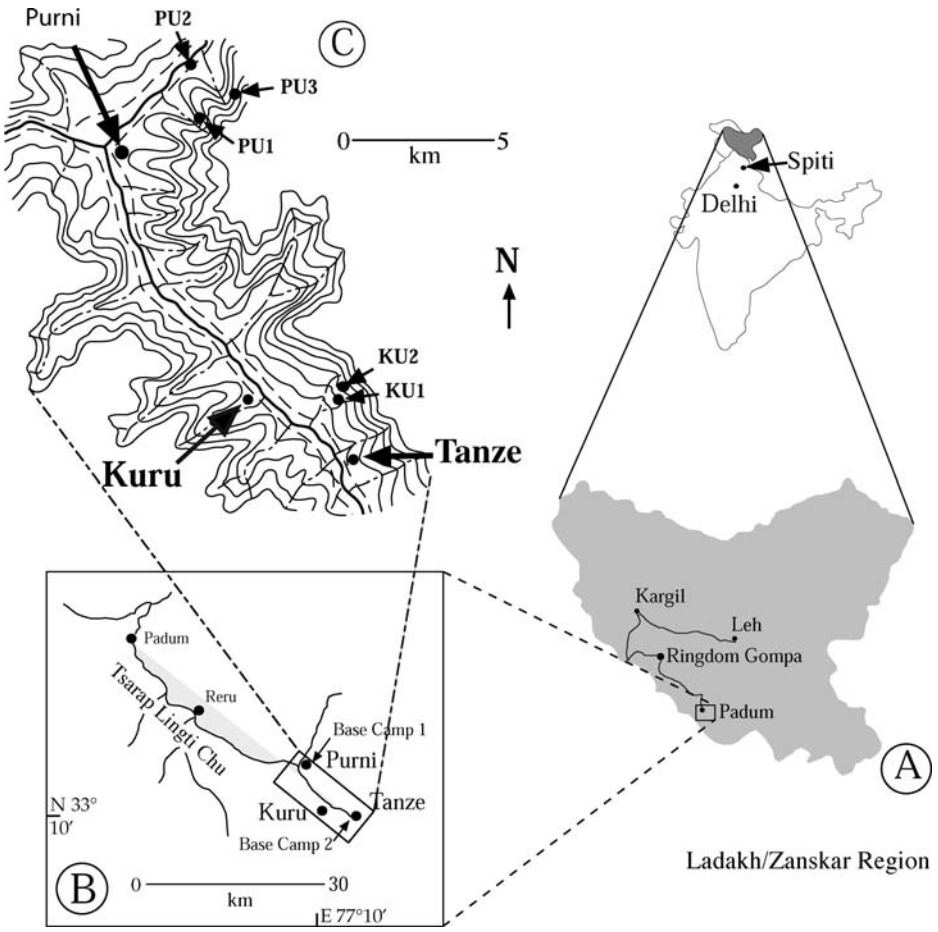

FIG. 1.—Location map of the study area. **A)** Ladakh district of northern India. **B)** Close-up of Tsarap Lingti River Valley. **C)** Topographic close-up map shows the locations of the five stratigraphic sections.

Greater and Tethyan Himalaya represent the basement and cover, respectively, of an exotic terrane accreted to India at the Cambrian–Ordovician boundary (DeCelles et al. 2000); and (3) Tethyan Himalayan Cambrian rocks formed part of the Indian shield but were deposited in an isolated basin separated by exposed basement of the "Central Crystalline Axis" (Saxena 1971; Aharon et al. 1987). These three models have fundamentally different implications about the Cambrian paleogeography of the equatorial peri-Gondwana region and the tectonic history of the Himalaya. A general biostratigraphic framework has been established for much of the Himalayan Cambrian (Jell and Hughes 1997; Hughes and Jell 1999; Hughes et al. 2005), but a modern process-oriented sedimentological analysis is required as a test of the Cambrian paleogeographic problems described above. In this study we present such an analysis for one of the most important and best-preserved Cambrian successions in the Himalaya, the Zanskar Valley section in Ladakh, northern India (Fig. 1).

The Zanskar region exposes a thick succession of Lower and Middle Cambrian strata of the Parahio Formation. Detailed study of the formation in this region, and in its type section in the Spiti valley of northern India (Fig. 2) (Myrow et al. in press), is critical for reconstruction of relationships between the Lesser and Tethyan Himalaya. In addition, Zanskar exposes younger dated Cambrian deposits (Karsha and Kurgiakh formations) than in Spiti and these may correlate in part or in whole with the youngest parts of the Cambrian of the Lesser Himalaya. These strata allow a more complete description of depositional history for the Himalayan region at this time. Further, these younger deposits have been interpreted to record a prominent transition from passive-margin deposition to active foreland-basin deposition during the Late Cambrian to Early Ordovician (Garzanti et al. 1986), associated with final assembly of core Gondwanaland. This study provides the first detailed paleoenvironmental analyses of these units, which is then used to evaluate the current tectonic model for Himalayan Cambrian–Ordovician orogenesis.

STRATIGRAPHY

The Cambrian rocks of Zanskar belong to the Haimanta Group. The Haimanta Group is a thick succession of sedimentary rocks that overlies crystalline rocks of the Greater Himalaya and terminates at an unconformity that separates Cambrian rocks from Middle Ordovician and younger deposits (Myrow et al. in press) (Fig. 2). Nanda and Singh (1976) first established a stratigraphic nomenclature for the Cambrian of the Zanskar Valley and defined the siliciclastic Phe Formation and the carbonate-rich Karsha Formation (Fig. 2). Garzanti et al. (1986) recognized the Kurgiakh Formation as a siliclastic unit conformably overlying the Karsha Formation and developed a series of members within each of the Phe, Karsha, and Kurgiakh Formations (Fig. 2). The boundary between the top of the Phe Formation and the base of the Karsha Formation was defined as the first rusty-weathering dolomite bed. In this paper we correlate the Parahio Formation of Spiti Valley (Fig. 2) with the entire Mauling Member of the Karsha Formation and possibly a small part of the upper Phe. This correlation is established on lithologic and biostratigraphic grounds. The name Parahio Formation has historical precedence and here is applied to this interval in the

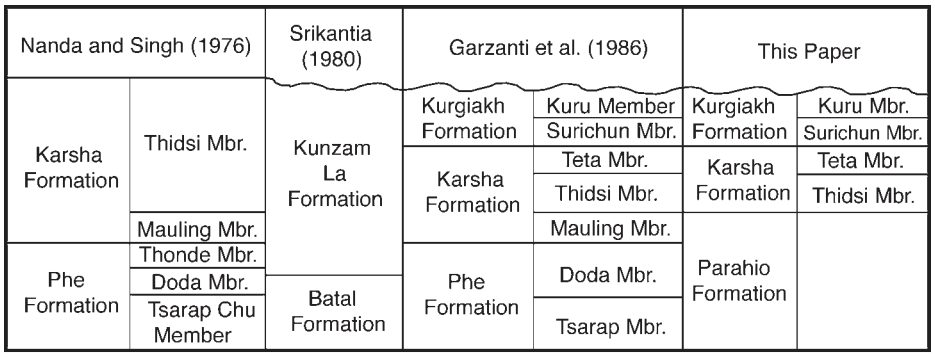

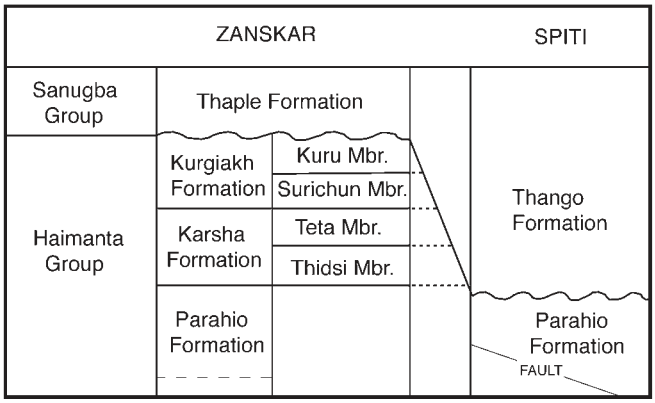

FIG. 2.—Upper box is a stratigraphic schemes for the Haimanta Group of the Zanskar Valley, India. Our stratigraphic revision is shown on the right. Lower box shows correlation between the stratigraphy of the Zanskar and Spiti Valley regions. Note cut-out of Kurgiakh and Karsha formations in Spiti.

Zanskar Valley for the first time. The top of the Parahio Formation in Zanskar is defined by the base of the thick carbonate of the Thidsi Member of the Karsha Formation (now restricted to only the Thidsi and Teta members).

The Parahio Formation at its type section in Spiti is differentiated from the underlying Batal Formation by the presence of carbonate beds, as well as trace and body fossils. Its base in the sections we studied in Zanskar is poorly resolved. The presence of red-weathering dolomite layers in the upper part of the type section of the Parahio Formation in Spiti was previously used to divide it into two members, but this criterion is of limited value because it is based on a diagenetic pattern that may be locally and/or regionally variable (Myrow et al. in press). In the Parahio Valley, limestone beds exist well below the level of the red-weathering dolomite beds to nearly the base of the formation.

In Zanskar, we place the contact between the Parahio Formation and the underlying Phe Formation at the first occurrence of trace fossils in the section, which occurs at the village of Purni as described by Hughes and Droser (1992). This is slightly beneath the first limestone bed in the succession, and is less than one hundred meters beneath the base of our measured section of the Parahio Formation. The first occurrence of trace fossils was also used to define the base of the Parahio Formation in Spiti. In Zanskar the siliciclastic rocks of the Phe Formation are more highly deformed than those of the overlying Parahio Formation, much as in Spiti, where the Batal Formation is markedly more deformed than the overlying Parahio Formation. Nanda and Singh (1976) cursorily defined several members of the Phe Formation, but the age of the clastic beds at Phe village (which we assume to be their unspecified type section of the Phe Formation) has yet to be established. It is unclear if these strata have distinctive lithofacies from the Parahio Formation because they are poorly preserved and detailed measured sections are not likely possible in these areas.

The Parahio Formation in Zanskar likely represents a relatively small part of the total thickness of the Haimanta Group, which may be up to 11 km thick in the Pir Panjal range of Kashmir (Draganits 2000). There, the lower part of the Haimanta Group contains the Manjir Formation, a conglomerate thought to correlate with the glaciogenic Blaini Formation of the Lesser Himalaya (Frank et al. 1995). The interval between the top of the Manjir Formation and the base of the Parahio Formation is estimated to be about 2500 meters thick and represents a mostly late Neoproterozoic succession. The names Phe Formation and Batal Formation (Srikantia et al. 1980) are commonly applied to these rocks. The type section of the Batal Formation is also poorly preserved, but detrital zircon grains (our unpublished data) indicate that some of the Batal Formation is Cambrian in age. Srikantia et al. (1980) applied the names Batal Formation and Kunzam La Formation to rocks in Zanskar, recognizing similarities between the two regions, but we have rejected the term Kunzam La Formation elsewhere (Myrow et al. in press).

PREVIOUS WORK

The presence of lower Paleozoic rocks in the Zanskar region was inferred by Lydekker (1883), who suggested that rocks of this age overlie the metamorphic rocks of the Greater Himalaya. The initial recognition of Cambrian rocks in Zanskar was based on trilobites illustrated by Dungrakoti et al. (1974) and Dungrakoti et al. (1977), and a lithostratigraphic nomenclature for the region was established by Nanda and Singh (1976) (Fig. 2). These authors did not designate type sections for the lithostratigraphic units or estimate their thicknesses, but they inferred that the Cambrian history of the Zanskar region commenced with deep-water flysch sedimentation (Phe Formation) followed by shallowing to peritidal conditions in the Karsha Formation. Fuchs (1987) proposed

a similar interpretation, as did Srikantia et al. (1980, p. 1015) who considered the lower Mauling Member of the Karsha Formation, herein assigned to the Parahio Formation (Fig. 2), as a deposit of a euxinic flysch basin that shallowed to carbonate shelf deposits of the middle and upper Karsha. Both Srikantia et al. (1980) and Nanda and Singh (1976) correlated orange dolostone beds in the Parahio Formation with equivalent beds in Spiti. Garzanti et al. (1986) considered the Parahio Formation to be dominated by tidal-flat deposits. They considered the Kurgiakh Formation to represent a sequence of basinal turbidites developed above the Karsha Formation as a response to tectonically induced subsidence associated with development of a foreland basin. Other workers (Gaetani et al. 1986) echoed this interpretation.

The dating of the Cambrian of Zanskar has been controversial. Early reports of trilobites (Dungrakoti et al. 1974, 1977; Srikantia et al. 1980) did not permit specific identification, and V.J. Gupta (Gupta and Shaw 1981, 1985; see Whittington 1986; Hughes and Droser 1992; Jell and Hughes 1997) spuriously reported a variety of lower Paleozoic Czech trilobites as being from the Cambrian of Zanskar. Confirmed reports of latest Middle Cambrian trilobites and trace fossils have been recorded from the Surichun Member of the Kurgiakh Formation from two localities (Whittington 1986; Jell and Hughes 1997; Hughes 2002), and a fauna of Middle Cambrian trilobites has been recovered from the upper part of the Parahio Formation in the Zanskar Valley (Shah et al. 1996; Kumar 1998). The trace fossil *Taphrhelminthopsis* cf. *circularis* was illustrated from the beds attributed to the Tsarap Member of the Phe Formation from Purni and interpreted as Lower Cambrian (Hughes and Droser 1992). However, as noted above, these strata are now assigned to the lower part of the Parahio Formation. Parcha (1998) figured other trace fossils from the Parahio Formation.

Thickness estimates for the lithostratigraphic units in Zanskar vary widely. Srikantia et al. (1980) estimated the Batal Formation to be 1700 m thick and the Kunzam La Formation (= all strata younger than Batal; Fig. 2) to be 2900 m thick, with the dolomite-bearing part to be about 1400 m thick. Garzanti et al. (1986) presented markedly different estimates, with the Phe Formation about 800 m thick, the Karsha Formation about 800 m thick, and the Kurgiakh Formation over 300 m thick. Fuchs (1987) estimated similar thicknesses for the upper units but thought that the Phe Formation was at least 2000 m thick. These disparate estimates illustrate some of the problems with the Cambrian lithostratigraphy of the Tethyan Himalaya.

LOCATION

The field area is located in the Zanskar Valley, in the District of Ladakh, northern India, State of Jammu and Kashmir (Fig. 1). The valley runs roughly NW–SE and is approximately 150 km to the SE of the town of Kargil, near the India–Pakistan border. Outcrops studied are located near the villages of Purni, Kuru, and Tanze in the Tsarap Lingti River Valley.

Three sections of the Parahio Formation were measured near Purni (PU1, PU2, PU3), roughly 1–2 km up the Niri River from the Purni base camp (Fig. 1). The three Purni sections have the following thicknesses: PU1 = 448.56 m, PU2 = 27.95 m, and PU3 = 602.54 m. The first section (PU1) represents the oldest well-preserved strata of the Parahio Formation. There is approximately 100 m of intensely faulted strata between PU1 and PU2 and 109.5 m of cover between PU2 and PU3.

The uppermost part of the Parahio Formation, the Thidsi and Teta members of the Karsha Formation, as well as the Kurgiakh Formation (Fig. 2), are exposed on the north side of Tsarap Lingti River, across from the town of Kuru. At this site, we measured a 37.2 m section through the Teta Member of the Karsha (KU1) and an 162.6 m section through the upper Kurgiakh Formation (KU2), the latter of which ends at the regional Cambrian–Ordovician unconformity. Coarse siliciclastic deposits of the Ordovician Thaple Formation overlie this unconformity.

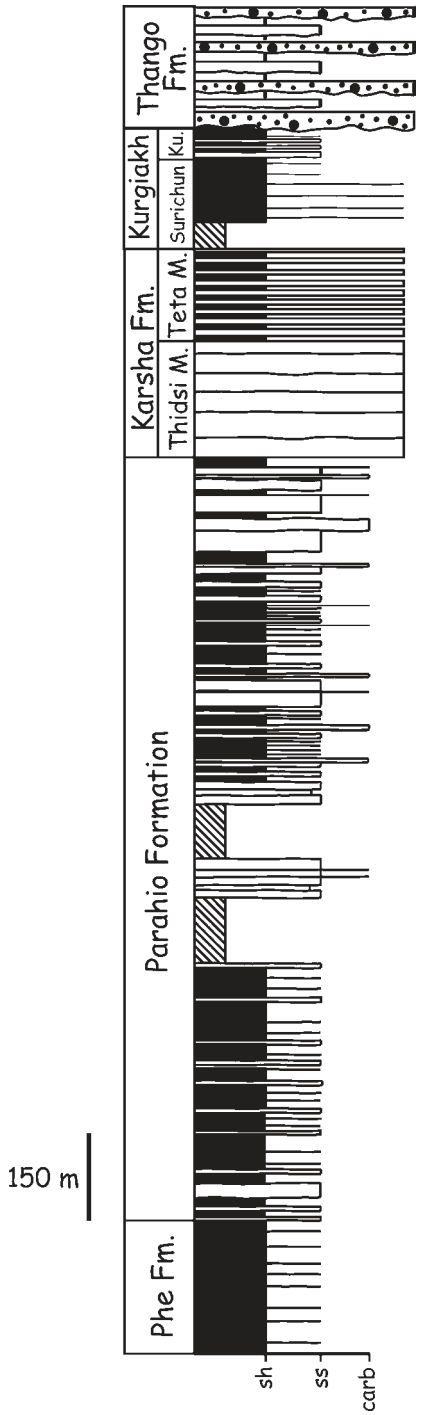

FIG. 3.—Stratigraphic section of lowermost Paleozoic strata of Zanskar Valley. Ku = Kuru Member. Grain-size scale at base: sh = shale, ss = fine sandstone, carb = carbonate.

FACIES ANALYSIS

At each of the five localities in the Tsarap Lingti River Valley, detailed bed-by-bed thickness measurements were made and sedimentary structures were identified and logged. A total of 1279 m were measured and described from all the sections (Fig. 3). Paleocurrent measurements were taken from many structures in each of the five sections, along with bedding orientations.

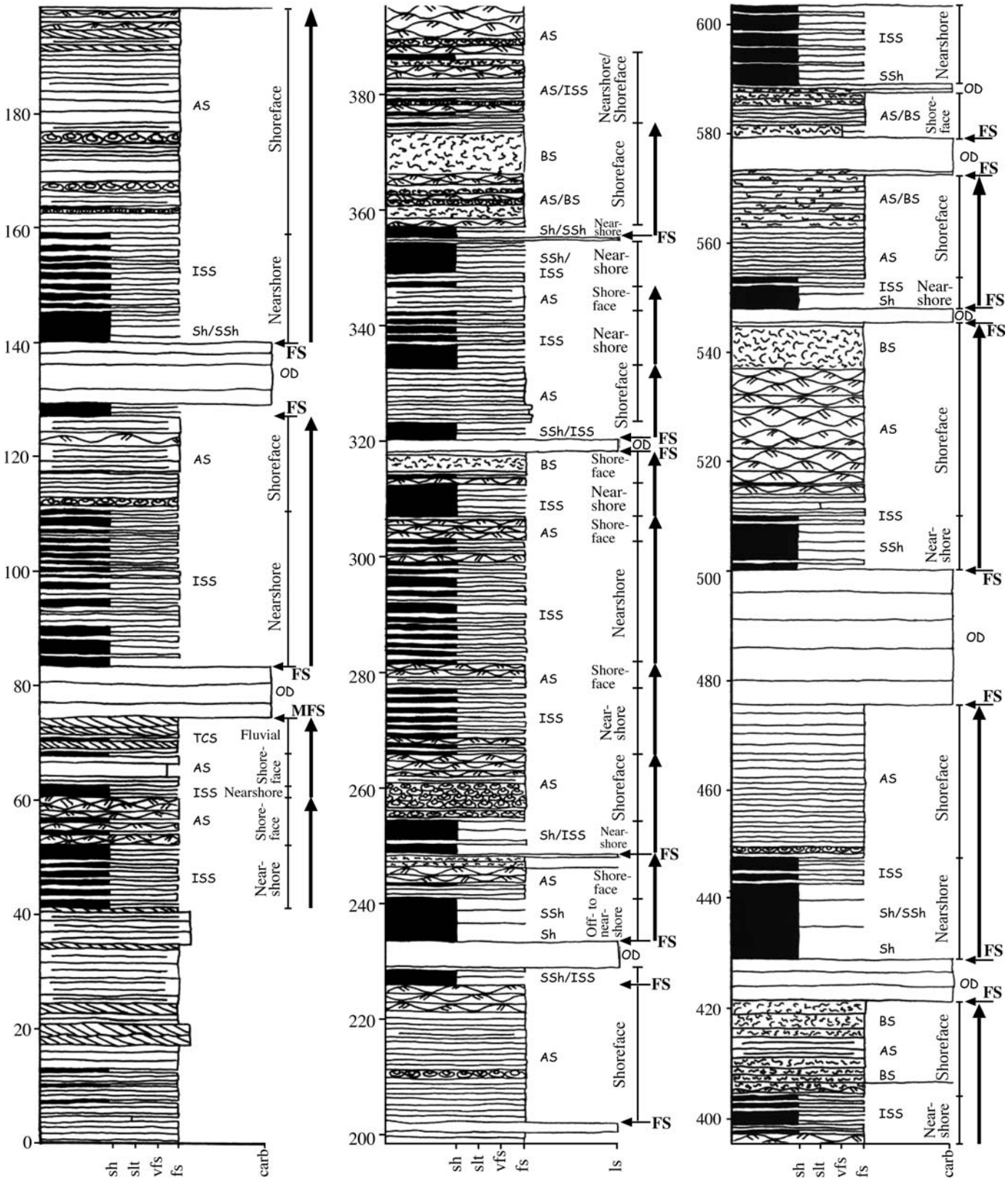

FIG. 4.— Detailed measured section at location PU3 (Fig. 1). Lithologic scale: sh = shale, slt = siltstone, vfs = very fine sandstone, fs = fine sandstone, carb = carbonate. Lithofacies described in text are shown to right of column: Sh = shale, SSh = Silt-streaked shale, ISS = Interbedded sandstone and shale, AS = Amalgamated sandstone, BS = Bioturbated sandstone, TCS = Trough cross-bedded sandstone, and OD = Orange dolostone. Flooding surfaces (FS), including marine flooding surfaces (MFS) that overlie fluvial cross-bedded sandstone, are shown with horizontal arrows. Thick vertical arrows delineate the stratigraphic distribution of upward-shoaling cycles.

FIG. 5.—Legend for Figures 4 and 11.

Eight lithofacies are defined for the approximately 1300-m-thick Parahio Formation. These lithofacies are in many cases arranged into cycles tens of meters thick with repeated stratigraphic patterns, which are shown in a detailed for section PU3 in Figure 4 (see legend in Fig. 5). The Thidsi Member of the Karsha Formation was not measured in detail due to time constraints. The Teta Member and the overlying Kurgiakh Formation both contain several lithofacies similar to those in the Parahio Formation, and we describe them separately using the lithofacies described below as a framework.

FACIES DESCRIPTIONS

Shale Facies

Description.—This facies is characterized by black to gray shale in beds up to 60 cm thick. The shale contains laminae of siltstone and very fine sandstone that constitute up to 20% of the facies. This facies commonly grades into the silt-streaked shale facies (described below). Medium to thick beds of this facies commonly directly overlie the orange dolostone facies. Lingulid brachiopods occur sparsely on some laminae.

Interpretation.—The shale, silt-streaked shale, and interbedded sandstone and shale facies represent a progression of increasing sandstone content and bed thickness. These facies contain moderately abundant burrows that indicate deposition in marine water. The low percentage of sandstone and siltstone in the shale facies implies an environment of very low energy, well below fair-weather wave base (FWWB). Accumulation of mud took place as a result of suspension deposition. The gray to black color reflects moderate to high organic-carbon content and generally low-oxygen diagenetic conditions (Savrda et al. 1984; Wignall and Myers 1988; Myrow 1990).

Silt-Streaked Shale Facies

Description.—This facies consists of gray-green silt-streaked shale interbedded with very fine to fine, very thin sandstone beds (Fig. 6). Siltstone and sandstone streaks occur as discontinuous laminae about 1 mm thick. Thicker sandstone beds from 1 to 4 cm thick are widely spaced within the silt-streaked shale, occurring about every 10–20 cm. This facies contains 20 to 50 percent siltstone and sandstone. Ripple cross-stratification and ripple form sets are common in this facies. Ripple form sets are generally symmetrical, and starved ripples are common (Fig. 6A). Burrowed zones up to 6 cm thick are also abundant, and individual burrow diameters range from 1 to 4 mm thick (Fig. 6B). Disarticulated trilobite sclerites are concentrated along laminae of this facies in the uppermost part of the Parahio Formation.

Interpretation.—The occurrence of siltstone streaks and thin sandstone beds in this shale-rich facies indicates an environment with episodic deposition of silt by both suspension and traction. The latter is indicated by the presence of small-scale symmetrical ripples, which reflect oscillatory currents and thus an environment above storm wave base (SWB). The orientations of starved-ripple crests indicate northwest–southeast oriented oscillatory flow. The relatively high percentage of siltstone and sandstone in this facies suggests a more proximal environment than the shale facies, presumably closer to fair-weather wave base (cf. Hamblin and Walker 1979).

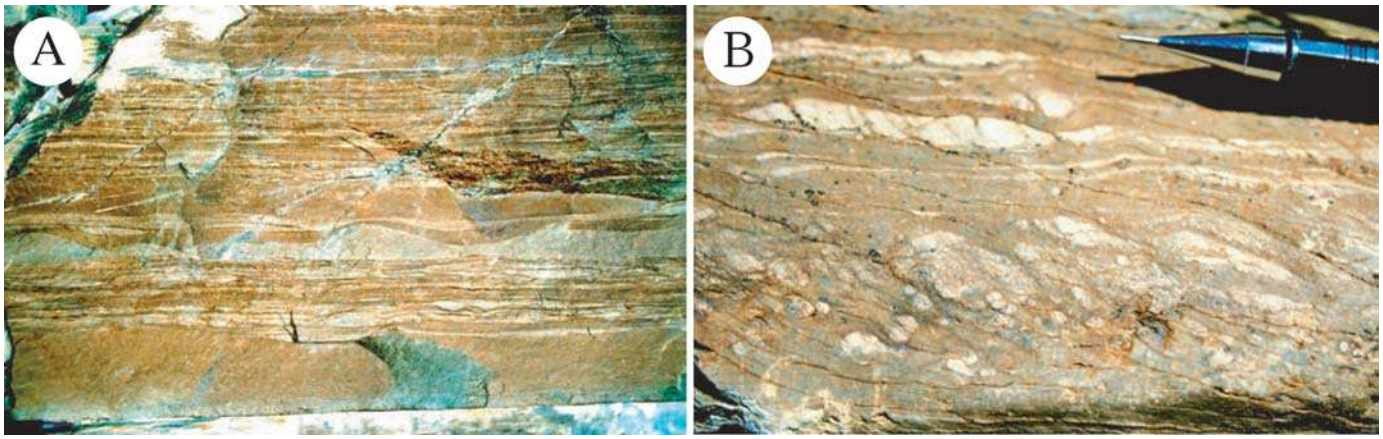

FIG. 6.—Silt-streaked shale facies. **A)** Dark, brown-weathered shale beds and tan-weathered siltstone beds at 260.42 m in PU1. Note the irregular and starved ripples. **B)** Burrows in the silt-streaked shale facies at 8.2 m in PU1.

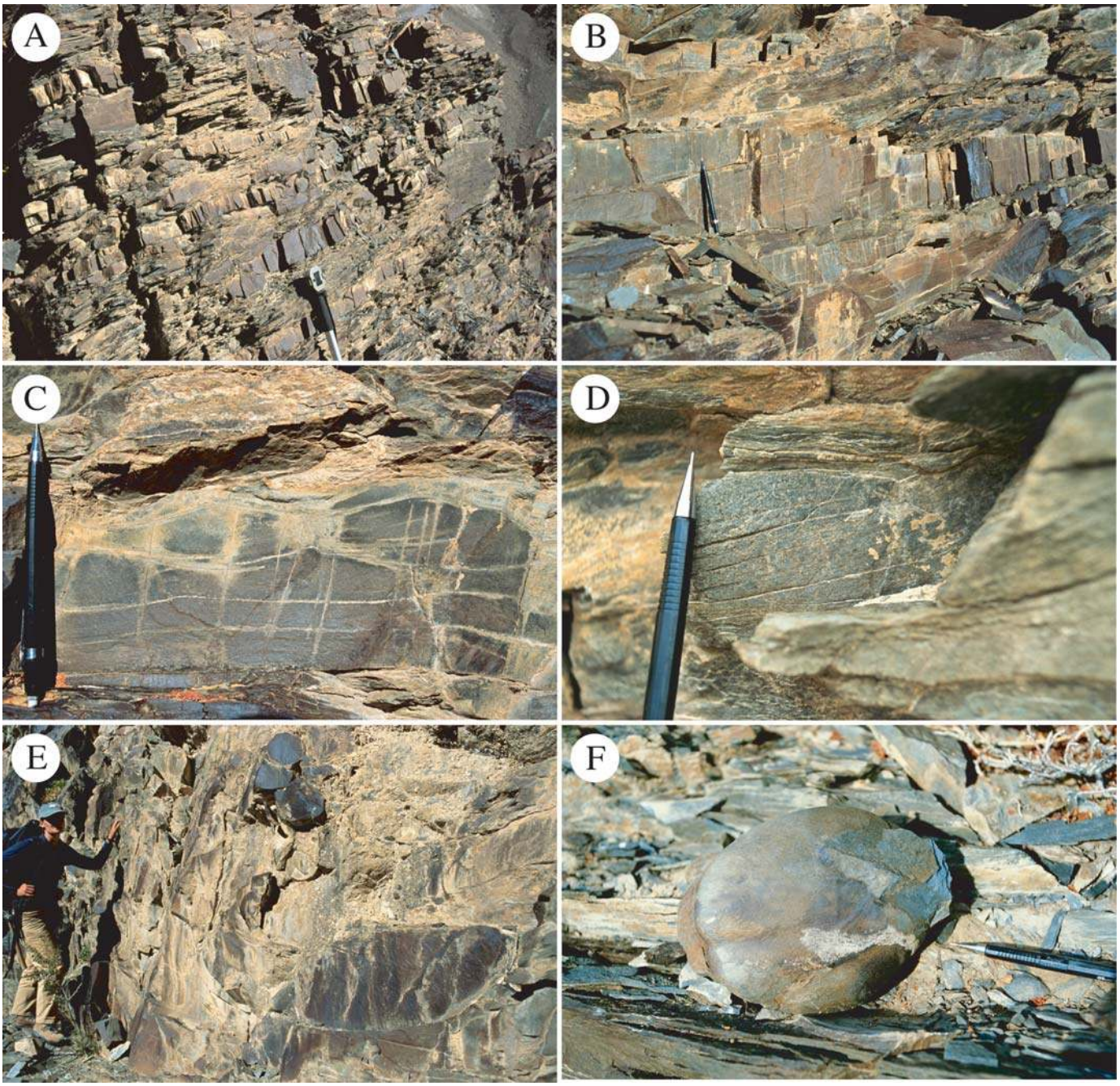

FIG. 7.— Interbedded sandstone and shale facies. **A)** Typical outcrop of the facies at ~ 400 m in PU3. Note layers of shale and thin to medium sandstone beds, Brunton compass for scale. **B)** Hummocky cross-stratification at 267.63 m in PU3. **C)** Wave-ripple cross-stratification at 272.17 m in PU3. **D)** Combined-flow ripple cross-stratification at 48.68 m in PU3. **E)** Large ball-and-pillow unit at 256.46 m in PU3. **F)** Excavated pot cast at 91.83 m in PU1. Pencil for scale is 13.5 cm long.

Interbedded Sandstone and Shale Facies

Description.—This facies consists of very thin- to medium-bedded sandstone and black to green-gray shale. Very fine to fine sandstone beds are 1 to 15 cm thick, and the shale beds are 2 to 20 cm thick. Some shale beds have burrows, and they vary in ichnofabric index from 1 to 5 (Droser and Bottjer 1986). The sandstone content throughout the section varies from approximately 50 to 80% sandstone (Fig. 7A). The sandstone beds contain parallel lamination, hummocky cross-stratification (HCS) (Fig. 7B), and ripple cross-stratification (Fig. 7C). Parallel lamination and HCS are common lower in the beds, and ripple-scale cross-lamination commonly caps the beds. Ripple form sets are both symmetrical and asymmetrical, the former with wavelengths from 3.5 to 9 cm and crest heights between 0.3 cm and 2 cm. The ripple cross-stratification also includes convex-up laminae and highly rounded ripple crests typical of combined-flow ripples (Yokokawa 1995; Myrow et al. 2002) (Fig. 7D). Gutter casts and pot casts occur sporadically in this facies (Fig. 7F). The elongation directions of the gutter casts indicate erosion by either northeast or southwest flow (Fig. 8A). The gutter casts typically have rounded U-shaped bases that are relatively symmetrical in cross section

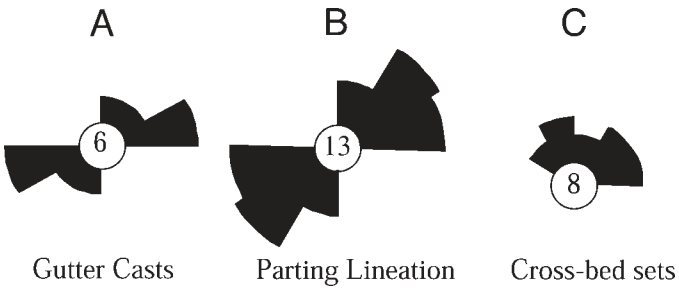

FIG. 8.—Paleocurrent data on the long axis orientations of **A)** gutter casts, **B)** parting lineations, and **C)** the foreset dip directions of dune-scale cross-bed sets.

and are mostly isolated from each other. One exhumed pot cast is a flattened spheroid with dimensions of 14 cm × 11 cm × 3 cm and an elongation direction northeast to southwest. The bases of many sandstone beds in this facies have groove marks, and the tops of some beds have mudcracks. Sandstone fills of mudcracks are typically less than 1 cm thick and in bedding plane view display mildly polygonal to sinuous, spindly patterns. Some of the thicker sandstone beds have ball-and-pillow structures 5 to 15 cm in diameter (Fig. 7E).

Interpretation.—The interbedded sandstone and shale facies contains features typical of storm-dominated shelf deposits. Wave ripples, combined-flow ripples, gutter casts, pot casts, hummocky cross stratification, and groove marks are all features resulting from higher energy, storm-generated, complex oscillatory and combined flows (Kreisa 1981; Whitaker 1973; Walker 1984; Arnott and Southard 1990; Myrow 1992a, 1992b). Vertical stratification sequences within individual beds (Myrow and Southard 1991) show evidence for flow deceleration, such as upper-plane-bed parallel lamination and HCS overlain by ripple-scale cross-lamination. Interbedded sandstone and shale with such features record deposition between FWWB and SWB along storm-dominated shorelines, and the shale beds (commonly bioturbated) record periods of quiet water suspension deposition (Dott and Bourgeois 1982; Walker 1984). The few scattered shrinkage cracks in this facies are anomalous and seem to contradict the inner shelf interpretation that we propose for this facies. However, the sinuous to spindly geometries of these features are consistent with their origin as diastasis (Cowan and James 1992) or synaeresis cracks (White 1961).

Amalgamated Sandstone Facies

Description.—This facies is composed of amalgamated very fine- to medium-grained sandstone beds from 5 to 15 cm thick (12 cm average). These amalgamated beds form bedsets that are up to 50 cm thick and separated by widely spaced thin (< 1 to 2 cm) shale partings (Fig. 9A, B). Very fine to fine sandstone beds are parallel laminated, quasi-planar laminated, and hummocky cross-stratified (Fig. 9). Medium sandstone beds contain only planar lamination. Hummocky cross-stratified and planar-laminated beds grade vertically into each other throughout this facies. Amalgamation surfaces on the tops of hummocky cross-stratified beds show irregular scours, and parting lineation occurs on exposed surfaces of many planar-laminated beds. Measurements taken from parting lineations indicate a northeast–southwest trend (Fig. 9B). Stacked ball-and-pillow structures up to 65 cm across are common in this facies, and constitute beds up to a few meters thick.

Interpretation.—The planar-laminated, quasi-planar-laminated, and hummocky cross-stratified amalgamated sandstone facies was also deposited under the influence of strong storm currents. The general absence of shale indicates that this facies was deposited above FWWB in a shoreface environment (Hamblin and Walker 1979). Stratification and other depositional structures of shoreface environments produced during fair-weather conditions are generally destroyed during storms (Dott and Bourgeois 1982). Planar lamination indicates deposition under upper-flow-regime plane-bed conditions, potentially ranging from purely unidirectional flow to purely oscillatory flow (Myrow and Southard 1996). Quasi-planar lamination results from deposition under combined flows just below the upper-plane-bed field (Arnott 1993). Some units with abundant planar lamination might in cases record swash and backswash processes typical of the adjacent foreshore environment (e.g., Carter 1978).

Bioturbated Sandstone Facies

Description.—This facies is characterized by very fine- to fine-grained bioturbated sandstone of ichnofabric index 5 (Droser and Bottjer 1986) (Fig. 10A). Beds range from 30 cm up to several meters thick. One 7-m-thick bed exists at 363.39 m of PU3 (Fig. 4). This facies is commonly transitional to the orange dolostone facies (described later) and is locally interbedded with the amalgamated sandstone facies and trough cross-bedded sandstone facies.

Interpretation.—The interbedding of the shoreface deposits of the amalgamated sandstone facies with this facies, and the lack of clay, including remnant shale beds, indicates deposition above FWWB also in a shoreface environment. Burrowing organisms reworked deposits that were likely amalgamated beds of sand and thus previously formed internal sedimentary structures such as HCS and parallel lamination were destroyed. It is unclear if intensely burrowed parts of the shoreface were a long-standing facies belt (i.e., lower shoreface where currents are less intense; Schwartz et al. 1997) or if they developed during particular episodes across part or all of the shoreface. Bioturbated sandstone is a common facies of both modern shorefaces (Howard and Reineck 1981; Schwartz et al. 1997) and ancient shoreface deposits (Carr et al. 2003; Castle et al. 2004).

Trough Cross-Bedded Sandstone Facies

Description.—This facies is characterized by medium to thick sets of fine- to medium-grained, trough cross-bedded sandstone. The sandstone in this facies weathers brown but is gray to light gray on unweathered surfaces. Cross-bed sets are 15 cm to 1.73 m thick, and they occur in cosets approximately 1 to 4 m thick (Fig. 10B, C). This facies is locally interbedded with the amalgamated sandstone facies. Paleocurrent measurements taken from the foresets of the trough cross-beds indicate north–directed paleoflow (Fig. 8C).

Interpretation.—The trough cross-bedded sandstone facies is locally interbedded with, but generally overlies, the storm-dominated deposits of the amalgamated sandstone facies. A Waltherian interpretation of the stratigraphic patterns would suggest that the facies was deposited landward of the shoreface and beach deposits of the amalgamated sandstone facies. The scale of the trough cross bedding indicates formation from migrating dunes that moved under unidirectional currents (Harms et al. 1982). Although there are relatively few paleocurrent readings (n = 8; Fig. 8), a larger number of readings (n = 25) from trough cross-bedded facies in similar cycles of the Parahio Formation from the Spiti Valley yield similarly uniformly northeast paleocurrents (Myrow et al. in press). The combination of

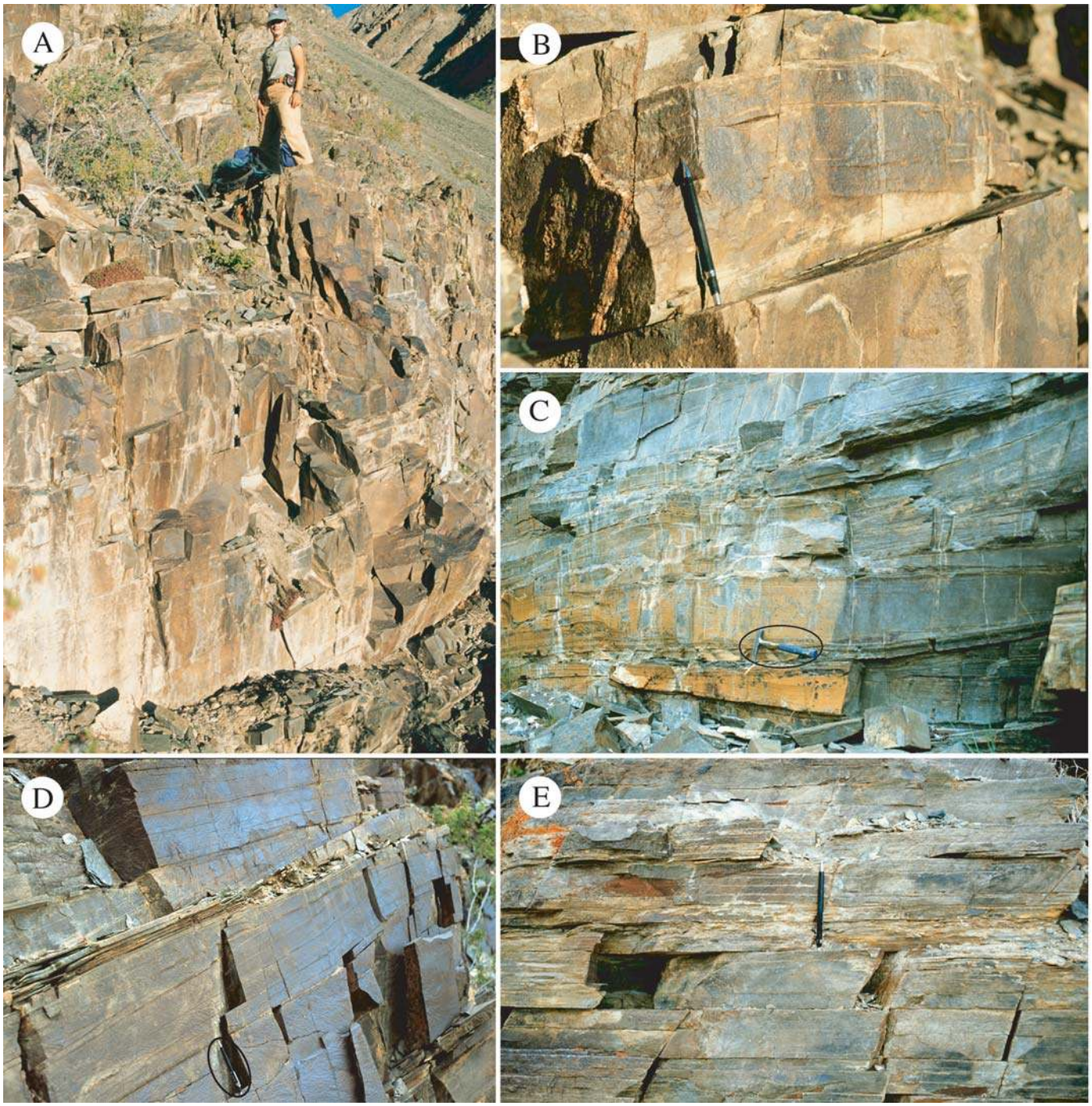

FIG. 9.— **A)** Upper part of a 6.2-m-thick unit of amalgamated HCS facies at 96.59 m in PU1. **B)** HCS bed with rounded hummock at 95.29 m in PU1. **C)** The amalgamated HCS facies at 6.88 m in PU2; hammer for scale. **D)** Quasi-planar laminated sandstone bed at 36.82 m in PU3. **E)** Amalgamated parallel-laminated sandstone bed at 2 m in PU3. Pencil for scale is 13.5 cm long.

unimodal paleocurrents, lack of body fossils or trace fossils, and a stratigraphic position above shoreline deposits in shoaling cycles is consistent with deposition in fluvial environments. The fine to medium sand grain size, and the lack of lags with large clasts, indicates that the river moved little coarse-grained sediment at its terminus into the ocean. Fluvial deposits that are dominated by dune-scale cross stratification and lack overbank fines are characteristic of sandy braided streams (Miall 1977; Godin 1991).

Orange Dolostone Facies

Description.—This facies is composed of orange-weathered dolomicrite and dolosiltite with minor grainstone beds (Fig. 10D, E). Units of this facies are 25 cm to 24.15 m thick and average about 6 m. In the thicker units, bedding planes are indistinct but typically spaced tens of centimeters apart. The facies is extremely uniform in appearance and displays few sedimentary structures. It locally contains thin grainstone

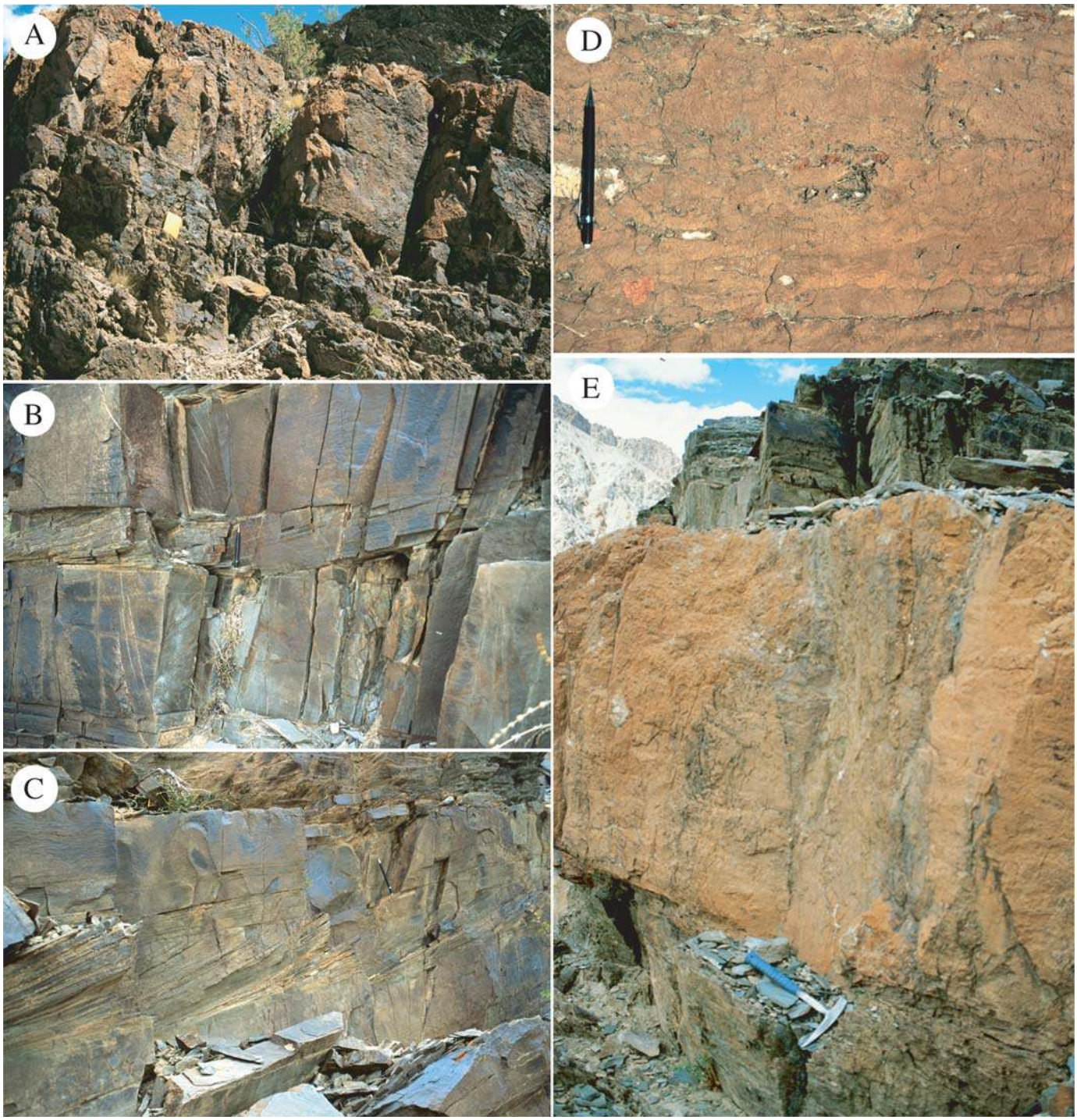

FIG. 10.—**A)** Thick unit of the bioturbated sandstone facies at from 315.09 m to 318.36 m in PU3. Notebook is 15 cm long. **B)** Dune-scale cross-bedding (center) at 17.21 m in PU3. **C)** Trough cross-bed set at 40.27 m in PU3. Pencil is 13.5 cm long. **D)** Close up of an orange dolostone bed of the carbonate facies at 421.61 m in PU3. **E)** Orange dolostone bed of the carbonate facies at 22.28 m in PU2. Hammer for scale.

beds, some of which contain intraclasts. Most dolostone beds overlie sandstone and sandstone-rich units and are commonly overlain by the black shale facies. Lingulid brachiopods are locally abundant.

Interpretation.—The dominantly micritic and homogeneous nature of the orange dolostone facies implies an environment of relatively low and uniform energy. The pure carbonate lithology and the occurrence of this facies above thick sandstone units in the cycles of the Parahio indicate a cessation of siliciclastic input, presumably within warm equatorial waters (cf. James and Kendall 1992). Paleomagnetic data indicate that the Tethyan Himalaya, the northern Indian margin at the time, was at equatorial latitude during the Cambrian (Scotese and McKerrow 1990) and would therefore have been amenable to widespread carbonate deposition in the absence of siliciclastic input. The presence of a few

grainstone beds in some units of this facies towards the top of PU3 indicates some minor variation of the energy level of the environment of deposition, but pervasive dolomitization and uniform texture make it impossible to accurately reconstruct the nature of the carbonate environments.

SEDIMENTARY CYCLES

The Parahio Formation has a series of upward-coarsening cycles that are similar to those identified by Myrow et al. (in press) in the same formation in the Spiti region. In Zanskar, these are best developed in the PU3 section (Fig. 4). Cycles range in thickness from approximately 12.4 to 62.2 m. An idealized cycle has the following succession of facies, from base to top: shale, silt-streaked shale, interbedded sandstone and shale, amalgamated sandstone or bioturbated sandstone, and trough cross-bedded sandstone. The overall trends developed in these facies transitions include upward decrease in shale, increase in sandstone, and increase in sandstone bed thickness. A bed of the orange dolostone facies caps an idealized cycle (Fig. 4, ~ 60–80 m). These carbonate beds are sharply overlain by the shale facies as the idealized cycle repeats.

However, such an idealized cycle rarely exists in its entirety. The bases are commonly not composed of the shale facies, but instead one of the succeeding facies such as the silt-streaked shale facies, interbedded sandstone and shale, bioturbated sandstone facies, or amalgamated sandstone facies (Fig. 4). In other cases, the cycles are not complete at the top and instead end in the fluvial, trough cross-bedded facies without a bed of orange dolostone (Fig. 4). The cycles may be even less complete and end in shoreface deposits of the amalgamated sandstone or bioturbated sandstone facies (Fig. 4).

PALEOENVIRONMENTAL INTERPRETATION

The interpretations of lithofacies given above indicate that the Parahio Formation was deposited along a storm-dominated shoreline and shelf, in which sediment was fed from a low-gradient sandy braided river system. This interpretation is consistent with that for the Parahio Formation in the nearby Spiti Valley (Myrow et al. in press). Such interpretations differ from that of Fuchs (1987), who interpreted the unit as a record of the infilling of a deep marine flysch basin. Garzanti et al. (1986) and Gaetani et al. (1986) suggested a shallow marine environment for the formation, but the local presence of mudcracks led them to interpret the Mauling Member (= Parahio Formation) as a tidal-flat deposit. This is inconsistent with the presence of a wide variety of storm-generated structures including HCS, the extreme paucity and ambiguous nature of the rare shrinkage cracks that are present, and the stratigraphic patterns and thicknesses of various lithofacies.

Interpretation of Cycles

On the basis of the paleoenvironmental interpretations, grain-size trends, and the succession of facies given above, these cycles clearly record repeated long-term shoaling events caused by progradation of a storm-dominated shoreline. The cycles reflect transitions from quiet mud-rich offshore environments to sandy shoreline then fluvial settings. In most cases, shoaling peaked with deposition of shoreface strata, but in a few cases ended with trough cross-bedded fluvial deposits. If the cycles were eustatically forced, both the scale of the cycles (10–60 m thick) and the total thickness of Middle Cambrian deposits (1,200–1,300 m) suggest that these would represent fourth-order depositional cycles (Haq et al. 1988). However, the cycles do not form regular stacking patterns—e.g., progradationally or retrogradationally stacked parasequences (Vail et al. 1977). This fact, the presence of abundant ball-and-pillow features, which reflect high sediment accumulation rates (Lindsay et al. 1984), and the presence of fluvial deposits at the top of some cycles, all suggest that these strata were deposited in a large-scale deltaic setting. The facies patterns and the irregular pattern of cycle thickness likely reflect episodes of shoreline progradation produced in large part by repeated switching of deltaic lobes (Penland et al. 1988). This interpretation follows that of Myrow et al. (in press) for similar cycles in the Parahio Formation in the Spiti region.

In the framework of a deltaic interpretation, the origin of the carbonate facies, which is linked to the cessation of siliciclastic input, would also potentially have been related to avulsion events within the delta. The transitions from fluvial sandstone into dolostone represent marine flooding surfaces (Van Wagoner et al. 1988) and the transitions from dolostone to deep-water shale are also flooding surfaces, but wholly marine and likely of greater magnitude. The presence of the carbonate facies above marine flooding surfaces and below upward-coarsening shoaling cycles indicates that the carbonate deposits represent thin transgressive systems tract (TST) deposits (Brown and Fisher 1977). The fact that carbonate beds rest on several different facies indicates that the carbonate was not a permanent facies belt but developed across flooded shoreface and coastal-plain deposits for a short term in response to the sudden reduction in input of terrigenous sediment. Flooding was presumably too rapid to allow the carbonate system to keep up with rising relative sea level (cf. Schlager 1981), which in this case was caused by the combination of high regional subsidence, produced at least in part by sediment loading within the delta complex (Coleman et al. 1983), and sudden reductions of sediment supply caused by avulsion. The decrease in sediment supply caused by avulsion allowed deposition of carbonate in nonturbid water during a short window in which the depositional surface would have been in shallow water, prior to resumption of siliciclastic input and progradation of a successive cycle. During deposition of a delta lobe, sediment supply presumably outstripped subsidence, and this resulted in shoreline progradation and upward-coarsening cycles.

The cycles described herein differ from those of the Parahio Formation in the Spiti Valley in that cycles in the Zanskar deposits are less well developed, contain fewer fluvial deposits, and generally contain more shale. These differences reflect variations in depositional setting along the length of the northern Indian margin at the time. The lower abundance of the trough cross-bedded sandstone facies in Zanskar relative to Spiti indicates that progradation did not progress to fluvial conditions as frequently in Zanskar. One possibility is that the Zanskar section was generally farther from the Tethyan shoreline of northern India relative to Spiti, and so only the most extreme progradational events would have progressed to fluvial conditions. This may reflect the fact that Zanskar, located north-northwest of Spiti, may have been in a more seaward position given that the purported strike of the Tethyan Cambrian paleoshoreline was generally oriented west-northwest (Brookfield 1993; Myrow et al. in press). Alternatively, the Zanskar Valley could have been in a region with less fluvial influence (i.e., fewer and smaller distributary channels). We are currently unable to determine whether the Zanskar and Spiti outcrop areas might record deposition from edge and axial parts of the same deltaic complex, respectively, or record two separate river systems with different levels of fluvial influence.

THIDSI AND TETA MEMBERS OF THE KARSHA FORMATION

The trend of increasing carbonate content in the upper Parahio Formation reached its culmination in the Thidsi Member. In every locality examined, either its lower or upper contact is a fault, so its true thickness is unknown. Preserved thicknesses are on the order of 100 to 125 m (Garzanti et al. 1986). The Thidsi Member is composed almost entirely of orange dolostone (Fig. 11A, see legend in Fig. 5) and records deposition in a clear-water carbonate-platform setting. Sedimentary structures are not well preserved in the dolostone, but large stromatolites are present at the base and top of the member (Fig. 11B). The transition from a deltaic

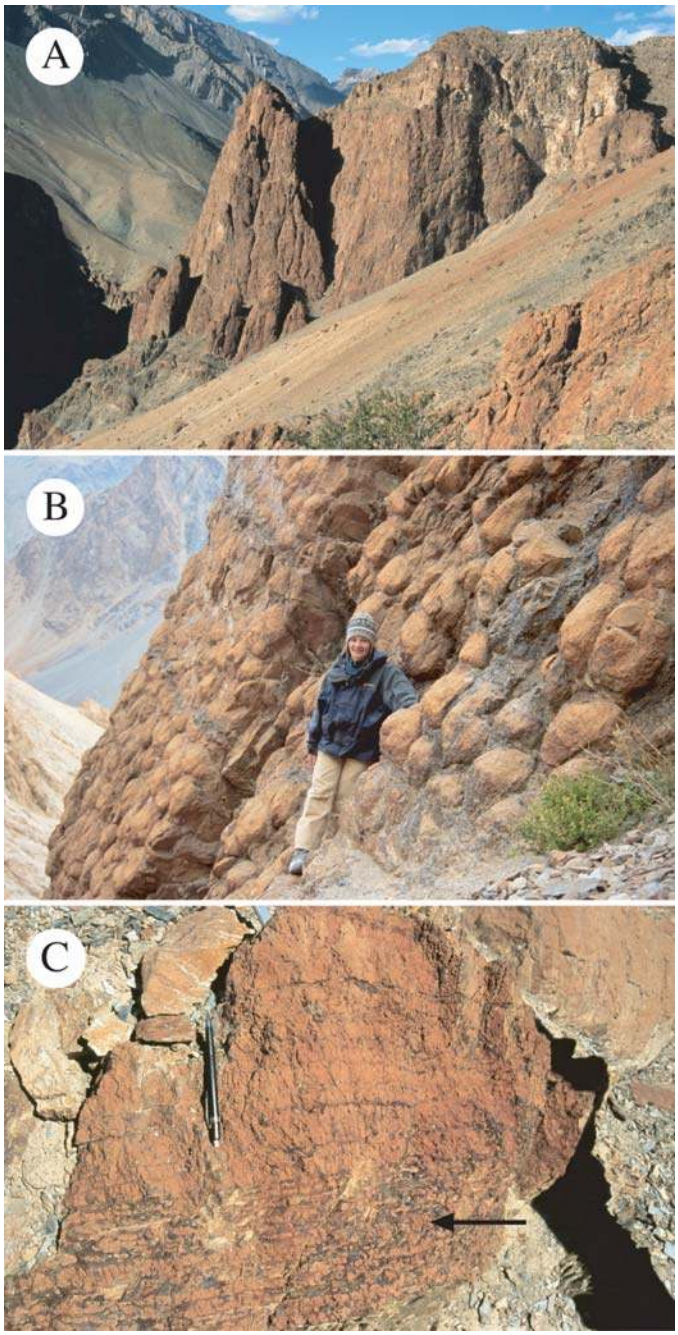

FIG. 11.— **A)** View of the > 100-m-thick Thidsi Member of the Karsha Formation from PU3. **B)** Stromatolite mounds at the top of a dolostone bed in the Thidsi Member, near the KU2 section. **C)** Dolostone bed at 3.59 m in the Teta Member. Arrow indicates chert stringers. Pencil is 13.5 cm long.

environment to a carbonate platform setting indicates a regional decrease in terrigenous sediment input that may have coincided with the reduction of hinterland topography and/or long-term climate change. This transition may represent the signal of part of a third-order (1–2 My) or second-order (up to 15 My) depositional sequence (Vail et al. 1977), as suggested by Myrow et al. (in press) for the Parahio in the Spiti Valley.

The Teta Member, a succession of thin to thick beds of orange dolostone, limestone, marl, and shale, gradationally overlies the uppermost Thidsi Member (Fig. 3). Dolomicrite and dolosiltite beds range from 4 to 66 cm thick and commonly contain chert concretions or stringers (Fig. 11C). Trilobites were collected from a number of thin limestone grainstone beds. White-weathered marl beds are 8 to 23 cm thick and are gradational with both dolostone and shale beds. Black-gray shale beds are 5 to 75 cm thick. At the top of the KU1 section, near the transition into the Surichun Member of the overlying Kurgiakh Formation, the shale is replaced in part by 5 to 25 cm thick green-gray, silt-streaked shale beds.

The lack of preserved sedimentary structures and the recrystallized nature of the dolostone make this unit difficult to interpret. Both components of this mixed siliciclastic–carbonate unit are fine grained, and so alternations of lithology may have been related to variations in siliciclastic input (possibly tied to climate) rather than episodic transport and deposition of the carbonate beds (cf. Sageman et al. 1997). The transition from the pure carbonate deposits of the Thidsi to the interbedded shale and dolostone of the Teta Member indicates a temporal increase in siliciclastic input, which continued in the overlying shale of the basal Kurgiakh Formation. The stratigraphic decrease in bed thickness and percent of carbonate likely reflects deepening and concomitant loss of primary carbonate production.

KURGIAKH FORMATION

The Kurgiakh Formation conformably overlies the Teta Member of the Karsha Formation and consists of the shale-rich Surichun Member and overlying mixed shale and sandstone deposits the Kuru Member. The formation contains lithofacies similar to those in the Parahio Formation. The Surichun Member is ~ 160 m thick opposite the town of Kuru, although the lower 48 m of the formation is covered and is presumably shale (Fig. 3). The middle and upper Surichun Member consists of black to gray shale, silt-streaked shale, and minor (< 10%) very thin to medium orange dolosiltite and dolomicrite beds with irregular chert stringers. The dolostone beds are 3 to 19 cm thick, and many of the thinner beds are highly nodular and may represent concretionary masses. Garzanti et al. (1986) report tuff beds up to 60 cm thick, but we noted none in the section at Kuru. They interpret trace-element data from the tuff beds to indicate a volcanic-arc basaltic source.

The Kuru Member is ~ 50 m thick and consists of interbedded sandstone and silt-streaked shale (Fig. 12). Silt-streaked shale beds range from 1 to 16 cm thick, and sandstone beds range from 6 to 81 cm thick. The sandstone beds are composed of clean, gray, very fine- to fine-grained, green-weathering quartz sand. According to Garzanti et al. (1986), the sandstone of the Kuru Member is quartzofeldspathic, contains < 1% lithic grains, and lacks carbonate clasts. They also report beds with classic Bouma T_{c-d} and T_{b-d} sequences. We found few graded beds, and none with classic turbidite structure. The sandstone beds instead contain abundant sedimentary structures, including hummocky cross stratification (HCS) (Fig. 13A–F), planar lamination, gutter casts (Fig. 14), ball-and-pillow structures, wave ripples, combined-flow ripples (Fig. 15), and minor graded bedding.

HCS and combined-flow ripples are well developed. The latter have features diagnostic of combined flow, namely highly rounded crests and convex-up laminae (Yokokawa 1995; Myrow et al. 2002) (Fig. 15). These ripples range in height from about 2 to 6 cm and have spacings of 18–24 cm. Sandstone beds in the Kuru Member also contain symmetrical ripples and typical wave-ripple lamination (DeRaaf et al. 1977) that includes features such as draping lamination, foresets that dip in different directions, and abundant scour surfaces. Paleocurrent data from the combined-flow ripples indicate current flow ranging from northeast to southeast; gutter casts are elongated northeast–southwest. Garzanti et al. (1986) reported intraclast-rich beds in which clast imbrication indicates NW transport.

The top of the Kurgiakh Formation is marked by a prominent, tectonically overprinted Cambrian–Ordovician unconformity. The over-

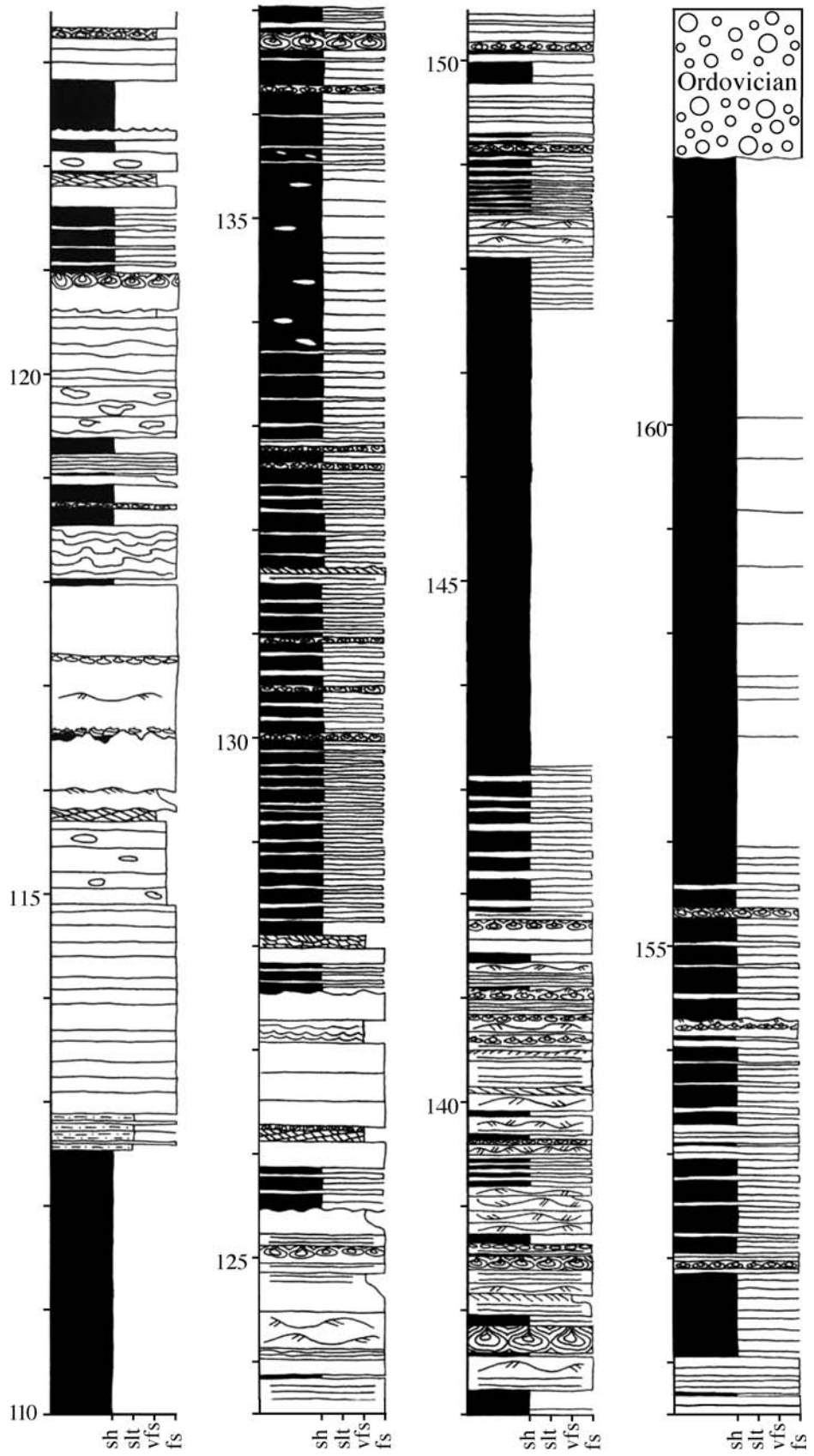

FIG. 12.—Stratigraphic column of the Kurgiakh Formation at the KU2 section. Section covers the upper 2.5 m of the Surichun Member and the entire Kuru Member. Lithologic scale: sh = shale, slt = siltstone, vfs = very fine sandstone, fs = fine sandstone. See Figure 4 for legend for symbols.

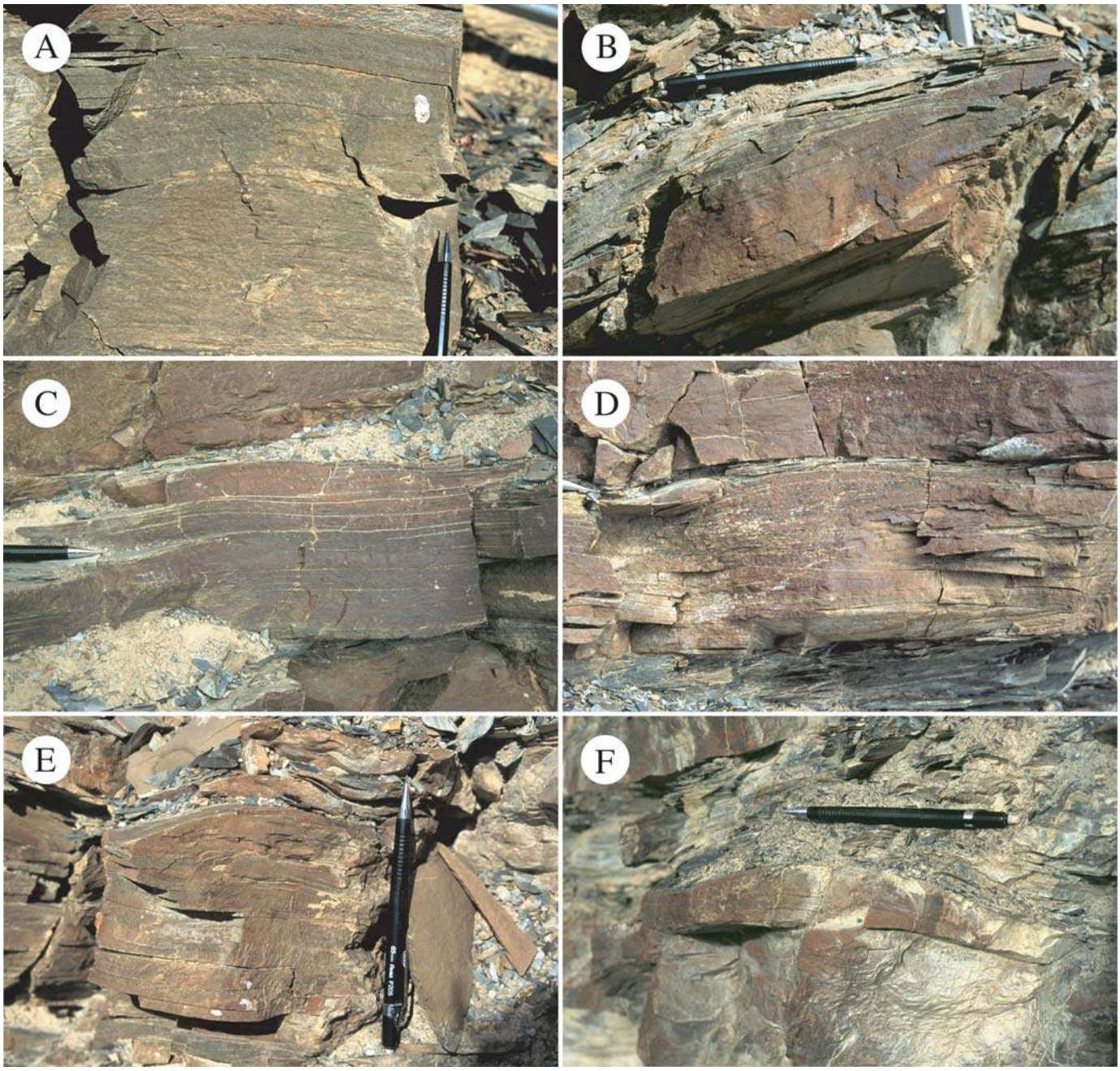

FIG. 13.—Hummocky cross stratified (HCS) sandstone in KU2. Pencil is 13.5 cm. **A)** Doming HCS lamination at 117.31 m. **B)** HCS at 137.22 m. **C)** Hummocky cross-stratified top of a 35-cm-thick parallel-laminated bed at 137.22 m. Note subtle low-angle curved erosion surfaces. **D)** HCS at 138.17 m. **E)** Small-scale hummock at 139.69 m. **F)** Low-relief, symmetrical hummock at 154.3 m.

lying Ordovician Thaple Formation consists of red conglomerate and sandstone and is comparable to the Thango Formation in the Spiti Valley. Petrographic study of the Thaple indicates litharenitic and sublitharenitic compositions. The lithic component is almost entirely siliciclastic and carbonate sedimentary grains (Garzanti et al. 1986).

Interpretation of the Kurgiakh Formation

The middle and upper parts of the Surichun Member are similar in lithology to the upper part of the underlying Teta Member of the Karsha Formation, although they contain less carbonate. The transition into the Kuru Member is relatively abrupt and shows upward coarsening into sandstone-dominated strata. The transition from the shale-rich middle Surichun Member to the Kuru Member reflects shoaling and progradation to inner-shelf and shoreline environments, as evidenced by abundant storm-generated structures such as HCS, combined-flow ripples, and gutter casts (Kreisa 1981; Myrow 1992a, 1992b). The bulk of the Kurgiakh Formation thus records long-term shoaling that followed the "Teta transgression." Maximum flooding of this preceding transgression may have been reached some time during deposition of the very poorly exposed lower Surichun Member.

Interbedded sandstone and shale deposits of the Kuru Member record deposition in the inner shelf, below fair-weather wave base, where mud

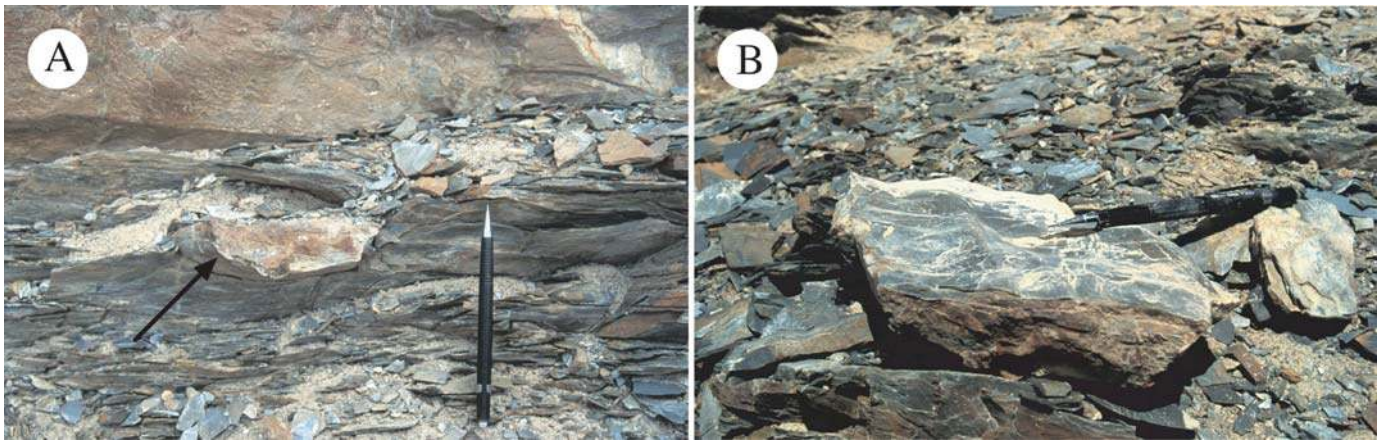

FIG. 14.—**A)** Gutter cast (arrowed) at 136.56 m in KU2. **B)** Oblique view of excavated gutter cast with symmetrical rippled top at 136.56 m in KU2. Pencil for scale is 13.5 cm.

settles out of suspension between storms (Walker 1984). The base of the Kuru consists of over 5 m of sandstone, and sandstone-rich intervals exist throughout the unit. These thick sandstone units, including those with amalgamated and nearly amalgamated HCS beds, represent shoreface and lower shoreface transition zone environments, respectively (cf. Dott and Bourgeois 1982).

Such an interpretation is at odds with previous views of the depositional and tectonic setting of this unit. According to Gaetani et al. (1986, p. 447–448), "the Kurgiakh Formation records the transition from shelf and slope sedimentation in poorly oxygenated waters to non-channelized distal turbidites. The sedimentary evolution thus testifies [to] active tectonic subsidence which largely exceeded sedimentation rates." Garzanti et al. (1986) consider the Surichun Member to record an upward transition from shelf to slope deposits and the Kuru Member as outer-fan-lobe turbidites and lobe-fringe deposits. They describe the depositional environment of the Kurgiakh Formation as "a restricted deep-water basin in front of an arc-trench system" (p. 261).

We agree with both Garzanti et al. (1986) and Gaetani et al. (1986) that the Teta Member of the Karsha Formation and the overlying Surichun Member of the Kurgiakh represent drowning of the Karsha carbonate platform, but this transgression was of limited extent and was followed by subsequent shoaling to inner-shelf and shoreline settings, not further deepening to slope and submarine-fan environments.

IMPLICATIONS FOR EARLY TECTONIC AND DEPOSITIONAL HISTORY OF THE NORTHERN INDIAN MARGIN

The Cambrian and Ordovician succession of the Zanskar region of northern India has been interpreted as recording the development of a foreland basin from a passive margin (Garzanti et al. 1986; Gaetani et al. 1986). This would include flexure and load-induced subsidence, drowning of a platform, development of a trench and deep-water trough, deposition of a turbidite succession, and late-stage collision and shedding of coarse molasse deposits. This interpretation has been used to support interpretations of other successions across the Tethyan Himalaya (e.g., Gehrels et al. 2003). Our sedimentological reinterpretation of these strata removes the fundamental premise for such an interpretation and casts considerable doubt on the purported genetic link between Kurgiakh sedimentation and the Cambrian–Ordovician orogenic event. First, the paleoenvironmental analysis of the Kurgiakh is inconsistent with deposition under extreme tectonic subsidence and development of a deep marine foreland basin. Second, as Garzanti et al. (1986) themselves point out, there is no peripheral-bulge unconformity (Beaumont et al. 1988) on top of the Karsha Formation and the sediment preserved in the Kurgiakh Formation lacks volcanic lithic fragments that would have been derived from a subduction complex.

Third, age relationships cast doubt on the published tectonic story. The youngest Cambrian faunas found below the Cambrian–Ordovician unconformity in the western Himalaya are found in Kashmir, where trilobites of earliest Late Cambrian age were recovered from the Trahagam Formation (Jell 1986; Jell and Hughes 1997). Beds above the boundary in Kashmir contain brachiopods (Reed 1934) that have recently been reinterpreted as no older than early Middle Ordovician age (L.R.M. Cocks, personal communication, 2004), or < 472 Ma (Gradstein et al. 2004). No fossils diagnostic of an Early Ordovician age have been found in the western Himalaya, and the oldest Ordovician fossils in Spiti appear to be no older than Middle Ordovician and no younger than Late Ordovician (L.R.M. Cocks and R.A. Fortey, personal communication, 2004). The hiatus associated with the unconformity between the Kurgiakh and the overlying Thaple Formation in Zanskar ranges from earliest Late Cambrian ($\sim$ 500 Ma) to Middle Ordovician ($\sim$ 472 Ma). In both Spiti and Zanskar, some coarse-grained continental deposits underlie the dated Ordovician strata, but there is nothing to suggest that these deposits are older than Middle Ordovician. Thus, the basal Ordovician unconformity might have developed at any time from earliest Late Cambrian to earliest Middle Ordovician, but most likely developed closer to the age of the oldest molasse deposits of the Tango and Thaple formations. In this case, tectonic uplift and erosion may have occurred roughly 20–30 million years after deposition of the Kurgiakh Formation. Thus, deposition of the Kurgiakh Formation, as well as the carbonate–siliciclastic transition at its base, could have significantly predated the Cambrian–Ordovician orogenic event.

The nature of Cambrian–Ordovician orogenesis is extremely poorly constrained due to lack of preserved rocks of this age in any Himalayan tectonic zones to the south of the South Tibetan Fault System (STFS), which separates the Tethyan Himalaya from the Greater Himalaya. Garzanti et al. (1986) suggest that uplifted Lesser Himalayan and Vindhyan strata could have been the source area for the Tethyan Ordovician deposits. Several problems arise from such an interpretation. First, there is little evidence for significant uplift within the Lesser Himalaya at this time. Hughes et al. (2005) point out that the uplift and erosion in the Lesser Himalaya occurred some time between the Late Cambrian and the Early Permian but that the timing of such an event within this interval is poorly constrained. There are also no structural fabrics or features yet identified as Cambrian or Ordovician in age in the Lesser Himalaya. Second, much of the Ordovician molasse deposits of the Tethyan Himalaya are coarse conglomeratic alluvial-fan and proximal

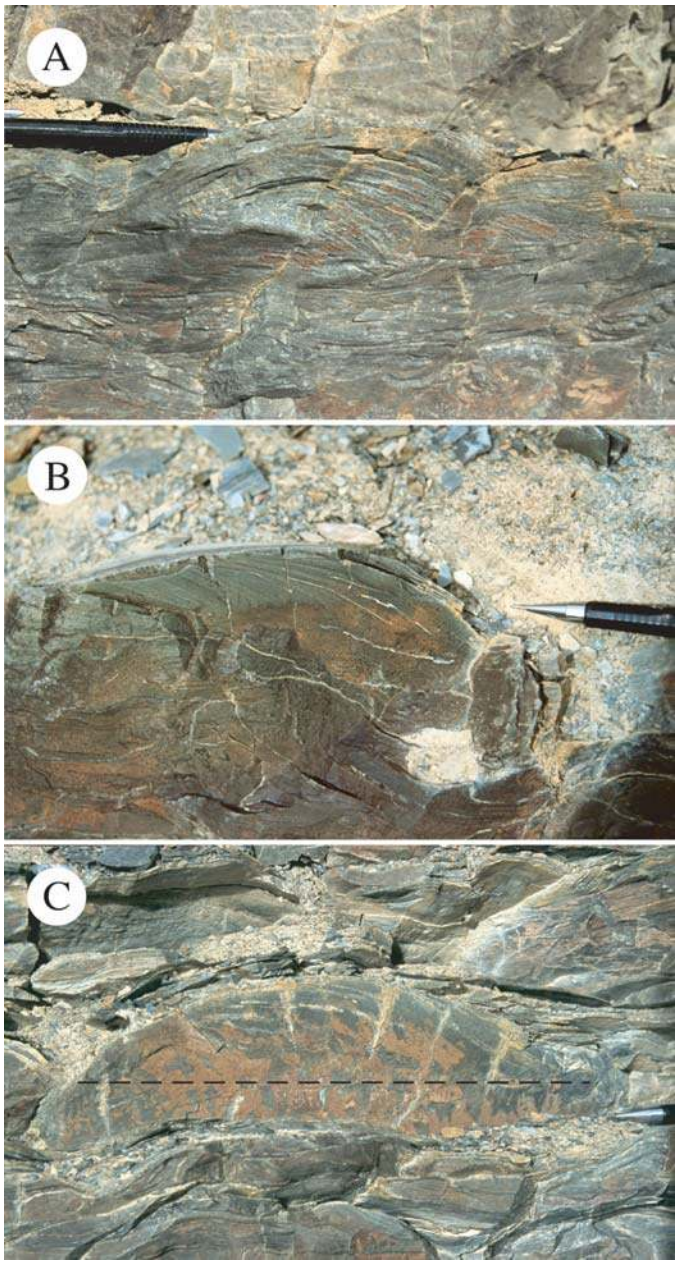

FIG. 15.—Combined-flow ripples in the Kurgiakh Formation at KU2. In each picture, note convex-up ripple structure and the highly rounded crests. Pencil is 13.5 cm long. **A)** Combined-flow ripple at 115.71 m. **B)** Combined-flow ripple at 150.12 m. **C)** Combined-flow ripple at 153.05 m. Cryptic break below ripple lamination is shown with dotted line.

fluvial deposits, which generally form adjacent to basin-margin faults. Although palinspastic reconstructions are somewhat ambiguous, they would not likely be compatible with extremely close juxtaposition of uplifted Lesser Himalayan or Vindhyan deposits with Tethyan sedimentary successions. The available data do not, however, argue against a Cambrian–Ordovician uplift south of the present-day STFS and the northern boundary of the Lesser Himalaya, the Main Central Thrust (MCT). In fact, paleocurrent data in the Ordovician strata of the Tethyan belt are consistent with this idea. As mentioned earlier, paleocurrent readings of cross-stratification in the Thaple Formation in Zanskar suggest eastward and subordinate northwest sediment transport directions (Garzanti et al. 1986). Paleocurrents from the Ordovician Tango Formation in the Spiti region (Bagati et al. 1991) indicate transport to the north and northeast, consistent with the orientation of meter-scale scours along its basal unconformity with the Parahio Formation (Myrow et al. in press). The strata in the paleogeographic region that would have represented the potential sediment source area for these Ordovician deposits are likely lost due to high-grade metamorphism and may now be represented in large part by Greater Himalayan crystalline rocks. Thus, the nature and existence of uplift in this region will likely remain a source of much speculation and debate unless important new structural and/or stratigraphic data become available.

In any case, the tectonic model outlined by Gehrels et al. (2003) is problematic with regard to the published paleocurrents for the coarse-grained Ordovician molasse deposits. Molassic deposits are typically shed in front of a fold-and-thrust belt, which in this case would be towards the south. Wedges of Ordovician molasse in Gehrels et al.'s (2003) reconstruction taper to the south and indicate southern progradation. We suggest that the application of standard models of foreland-basin development to Cambrian–Ordovician orogenesis in the Himalayas, such as those presented by Garzanti et al. (1986) and Gehrels et al. (2003), are premature and not justified by available data.

CONCLUSIONS

1. The Cambrian Parahio Formation in the Zanskar Valley consists of ~ 1,300 m of dominantly siliciclastic marine Cambrian deposits. The formation consists of cyclically deposited, storm-influenced, shoaling cycles that record environments that range from offshore marine to shoreface to fluvial environments. Carbonate beds that cap these cycles are thin transgressive deposits. These interpretations are at odds with previous paleoenvironmental interpretations that ranged from deep-sea flysch to intertidal.
2. Similar cycles exist in the Parahio Formation to the south-southeast at its type section in the Spiti Valley, although facies analysis of the Zanskar cycles indicate more distal paleoenvironments than their equivalents in Spiti. Trilobite and brachiopod faunas from both localities provide the first detailed correlations between these areas.
3. Paleocurrent data for marine and fluvial facies of the Parahio Formation in both Zanskar and Spiti indicate northeast sediment transport. This supports the view that the Parahio and overlying carbonate of the Karsha Formation record the ancient northern passive margin of India during the Cambrian. These strata may represent distal equivalents of the younger Cambrian deposits of the Lesser Himalaya.
4. The Cambrian succession is capped by the Kurgiakh Formation, a dominantly siliciclastic upward-coarsening unit that is overlain by a regionally extensive unconformity and overlying Ordovician conglomerate. The Kurgiakh Formation has been thought to represent a transition from a passive-margin to deep-water flysch deposition in a tectonically active foreland basin next to an arc-trench system. Purported sandstone turbidite beds with classic Bouma sequences are a key to this interpretation. We herein demonstrate that the Kurgiakh event beds contain well-developed hummocky cross-stratification, quasi-planar lamination, and combined-flow ripple stratification, which indicate that they were deposited in shallow-marine, storm-influenced environments. Although subsidence was substantial enough and rapid enough to drown the Karsha carbonate platform, it did not culminate in deep-sea flysch deposition.
5. Several other aspects of Cambrian–Ordovician deposits of northern India cast doubt on the proposed link between Kurgiakh sedimentation and the Cambrian–Ordovician orogenic event. First, the age gap between the youngest Cambrian strata and oldest

Ordovician strata indicate that the Kurgiakh may have been deposited as much as 20–30 My prior to the Ordovician conglomeratic molasse. Second, data from the Ordovician molasse indicate northward paleocurrents, which are at odds with models of standard foreland-basin development for the Cambrian–Ordovician event.

ACKNOWLEDGMENTS

We thank O.N. Bhargava and Eric Draganits for discussions of the Tethyan stratigraphy, and associate editor Sanjeev Gupta and an anonymous reviewer for helpful reviews. Field support was provided through the Wadia Institute of Himalayan Geology. Our Himalayan research is supported by National Science Foundation grant EAR-9980376 to PMM and EAR-9980426 to NCH, and by National Geographic grant NGS7293-02 to NCH.

REFERENCES

Aharon, P., Schidlowski, M., and Singh, I.B., 1987, Chronostratigraphic markers in the end-Precambrian carbon isotope record of the Lesser Himalaya: Nature, v. 327, p. 699–702.

Arnott, R.W., 1993, Quasi-planar-laminated sandstone beds of the Lower Cretaceous Bootlegger Member, north-central Montana: evidence of combined-flow sedimentation: Journal of Sedimentary Petrology, v. 63, p. 488–494.

Arnott, R.W., and Southard, J.B., 1990, Exploratory flow-duct experiments on combined-flow bed configurations, and some implications for interpreting storm-event stratification: Journal of Sedimentary Petrology, v. 60, p. 211–219.

Bagati, T.N., Kumar, R., and Ghosh, S.K., 1991, Regressive–transgressive sedimentation in the Ordovician sequence of the Spiti (Tethys) basin, Himachal Pradesh, India: Sedimentary Geology, v. 73, p. 171–184.

Beaumont, C., Quinlan, G., and Hamilton, J., 1988, Orogeny and stratigraphy: Numerical models of the Paleozoic in the eastern interior of North America: Tectonics, v. 7, p. 389–416.

Brookfield, M.E., 1993, The Himalayan passive margin from Precambrian to Cretaceous times: Sedimentary Geology, v. 84, p. 1–35.

Brown, L.F., and Fisher, W.L., 1977, Seismic–stratigraphic interpretations of depositional systems: examples from Brazil rift and pull-apart basins, *in* Payton, C.E., ed., Seismic Stratigraphy—Applications to Hydrocarbon Exploration: American Association of Petroleum Geologists, Memoir 26, p. 213–248.

Carr, I.D., Gawthorpe, R.L., Jackson, C.A.L., Sharp, I.R., and Sadek, A., 2003, Sedimentology and sequence stratigraphy of early syn-rift tidal sediments: the Nukhul Formation, Suez Rift, Egypt: Journal of Sedimentary Research, v. 73, p. 407–420.

Carter, C.H., 1978, A regressive barrier and barrier-protected deposit: depositional environment and geographic setting of the Late Tertiary Cohansey Sand: Journal of Sedimentary Petrology, v. 48, p. 933–950.

Castle, J.W., Molz, F.J., Lu, S., and Dinwiddie, C.L., 2004, Sedimentology and fractal-based analysis of permeability data, John Henry Member, Straight Cliffs Formation, (Upper Cretaceous), Utah, U.S.A.: Journal of Sedimentary Research, v. 74, p. 270–284.

Coleman, J.M., Prior, D.B., and Lindsay, J.F., 1983, Deltaic influences on shelf edge instability processes, *in* Stanley, D.J., and Moore, F.T., eds., The Shelf break: Critical Interface on Continental Margins: SEPM, Special Publication 33, p. 121–137.

Corfield, R.I., and Searle, M.P., 2000, Crustal shortening estimates across the north Indian continental margin, Ladakh, NW India, *in* Khan, M.A., Treloar, P.J., Searle, M.P., and Jan, M.Q., eds., Tectonics of the Nanga Parbat Syntaxis and the Western Himalaya: Geological Society of London, Special Publication 170, p. 395–410.

Cowan, C.A., and James, N.P., 1992, Diastasis cracks: mechanically generated synaeresis-like cracks in Upper Cambrian shallow water oolite and ribbon carbonates: Sedimentology, v. 39, p. 1101–1118.

DeCelles, P.G., Gehrels, G.E., Quade, J., Lareau, B., and Spurlin, M., 2000, Tectonic implications of U–Pb zircon ages of the Himalayan Orogenic belt in Nepal: Science, v. 288, p. 497–499.

DeRaaf, J.F.M., Boersma, J.R., and Van Gelder, A., 1977, Wave-generated structures and sequences from a shallow marine succession, Lower Carboniferous, County Cork, Ireland: Sedimentology, v. 4, p. 1–52.

Dott, R.H, Jr., and Bourgeois, J., 1982, Hummocky stratification: Significance of its variable bedding sequences: Geological Society of America, Bulletin, v. 93, p. 663–680.

Draganits, E., 2000, The Muth Formation in the Pin Valley (Spiti, N. India): Depositional environment and ichnofauna of a Lower Devonian barrier island system [Ph.D. thesis]: Vienna, University of Vienna, 165 p.

Droser, M.L., and Bottjer, D.J., 1986, A semiquantitative field classification of ichnofabric: Journal of Sedimentary Petrology, v. 56, p. 558–559.

Dungrakoti, B.D., Das, B.K., and Sinha, P.K., 1977, Record of additional fossils from the formation of Zanskar, Ladakh District, Jammu and Kashmir: Records of the Geological Survey of India, v. 109, p. 161–165.

Dungrakoti, B.D., Sinha, P.K., and Das, B.K., 1974, Trilobites from the Zanskar Valley, Ladakh District, Jammu and Kashmir State: Indian Minerals, v. 28, p. 114–115.

Frank, W., Grasemann, B., Guntli, P., and Millier, C., 1995, Geological map of the Kishtwar, Chamba, and Kulu region, NW Himalaya, India: Austria, Geologische Bundesanstalt, Jahrbuch, v. 138, p. 299–308.

Fuchs, G., 1987, The Geology of Southern Zanskar (Ladakh)—Evidence for the Autochthony of the Tethys Zone of the Himalaya: Austria, Geologische Bundesanstalt, Jahrbuch, v. 124, p. 325–359.

Gaetani, M., Casnedi, R., Fois, E., Garzanti, E., Jadoul, F., Nicora, A., and Tintori, A., 1986, Stratigraphy of the Tethys Himalaya in Zanskar, Ladakh: Rivista Italiana di Paleontologia e Stratigraphia, v. 48, p. 237–265.

Garzanti, E., Casnedi, R., and Jadoul, F., 1986, Sedimentary Evidence of a Cambro–Ordovician Orogenic Event in the Northwestern Himalaya: Sedimentary Geology, v. 48, p. 237–265.

Gehrels, G.E., DeCelles, P.G., Martin, A., Ojha, T.P., Pinhassi, G., and Upreti, B.N., 2003, Initiation of the Himalayan orogen as an early Paleozoic thin-skinned thrust belt: GSA Today, v. 13, no. 9, p. 4–9.

Godin, P.D., 1991, Fining-upward cycles in the sandy braided-river deposits of the Westwater Canyon Member (Upper Jurassic), Morrison Formation, New Mexico: Sedimentary Geology, v. 70, p. 61–82.

Gradstein, F.M., and others, 2004, A Geologic Time Scale 2004: Cambridge University Press, 589 p.

Gupta, V.J., and Shaw, F.C., 1981, Lower Palaeozoic trilobites from Ladakh Himalaya, India: Recent Researches in Geology, v. 8, p. 54–65.

Gupta, V.J., and Shaw, F.C., 1985, Lower Palaeozoic trilobites from Zanskar Valley, Ladakh, Himalaya, India: Research Bulletin (Science) of the Panjab University, v. 36, p. 335–344.

Hamblin, A., and Walker, R.G., 1979, Storm-dominated shallow marine deposits: the Fernie–Kootenay (Jurassic) transition, southern Rocky Mountains: Canadian Journal of Earth Sciences, v. 16, p. 1673–1690.

Haq, B.U., Hardenbol, J., and Vail, P.R., 1988, Mesozoic and Cenozoic chronostratigraphy and cycles of sea-level change, *in* Wilgus, C.K., Hastings, B.S., Kendal, C.G, St.C., Posamentier, H.W., Ross, C.A., and Van Wagoner, J.C., eds., Sea-level Changes—An Integrated Approach: SEPM, Special Publication 42, p. 71–108.

Harms, J.C., Southard, J.B., and Walker, R.G., 1982, Structures and Sequences in Clastic Rocks: SEPM, Short Course 9, 249 p.

Howard, J.D., and Reineck, H.E., 1981, Depositional facies of high energy beach to offshore sequences: Comparison with low energy sequences: American Association of Petroleum Geologists, Bulletin, v. 65, p. 807–830.

Hughes, N.C., 2002, Late Middle Cambrian trace fossils from the Lejopyge armata horizon, Zanskar Valley, India and the use of Precambrian/Cambrian lithostratigraphy in the Indian subcontinent, *in* P.N. Wyse Jackson, M.A. Parkes, R. Wood, and D.J. Batten, eds., Studies in Palaeozoic Palaeontology and Biostratigraphy in Honour of Charles Hepworth Holland: Special Papers in Palaeontology, v. 67, p. 135–151.

Hughes, N.C., and Droser, M.L., 1992, Trace fossils from the Phe Formation (Lower Cambrian), Zanskar Valley, northwestern India: Queensland Museum, Memoirs, v. 32, p. 139–144.

Hughes, N.C., and Jell, P.A., 1999, The biostratigraphy and biogeography of Himalayan Cambrian trilobites, *in* Macfarlane, A., Sorkhabi, R.B., and Quade, J., eds., Himalaya and Tibet: Mountain Roots to Mountain Tops: Geological Society of America, Special Paper 328, p. 109–116.

Hughes, N.C., Peng, S.-C., Bhargava, O.N., Ahulwalia, A.D., Walia, S., Myrow, P.M., and Parcha, S.K., 2005, Early Tsanglangpuan (late Early Cambrian) trilobites from the Nigali Dhar syncline and the Cambrian biostratigraphy of the Tal Group, Lesser Himalaya, India: Geological Magazine, v. 142, p. 57–80.

James, N.P., and Kendall, A.C., 1992, Introduction to carbonate and evaporite facies models, *in* Walker, R.G., and James, N.P., eds., Facies Models: Response to Sea Level Change: Geological Association of Canada, p. 265–275.

Jell, P.A., 1986, An early Late Cambrian trilobite faunule from Kashmir: Geological Magazine, v. 123, p. 487–492.

Jell, P.A., and Hughes, N.C., 1997, Himalayan Cambrian trilobites: Special Papers in Palaeontology, v. 58, p. 1–113.

Kreisa, R.D., 1981, Storm-generated sedimentary structures in subtidal marine facies with examples from Middle and Upper Ordovician of southwestern Virginia: Journal of Sedimentary Petrology, v. 51, p. 823–848.

Kumar, A., 1998, Record of well preserved trilobites from the Zanskar Valley: Geological Society of India, Journal, v. 51, p. 671–678.

Lindsay, J.F., Prior, D.B., and Coleman, J.M., 1984, Distributary mouth bar development and role of submarine landslides in delta growth, South Pass, Mississippi Delta: American Association of Petroleum Geologists, Bulletin, v. 68, p. 1724–174.

Lydekker, R., 1883, The geology of Kashmir and Chamba territories and the British district of Kangan: Geological Survey of India, Memoirs, v. 22, p. 1–344.

Miall, A.D., 1977, A review of the braided river depositional environment: Earth-Science Reviews, v. 13, p. 1–62.

Myrow, P.M., 1990, A new graph for understanding colors of mudrocks and shales: Journal of Geological Education, v. 38, p. 16–20.

Myrow, P.M., 1992a, Bypass-zone tempestite facies model and proximality trends for an ancient muddy shoreline and shelf: Journal of Sedimentary Petrology, v. 62, p. 99–115.

Myrow, P.M., 1992b, Pot and gutter casts from the Chapel Island Formation, Southeast Newfoundland: Journal of Sedimentary Petrology, v. 62, p. 992–1007.
Myrow, P.M., and Southard, J.B., 1991, Combined-flow model for vertical stratification sequences in shallow marine storm-deposited beds: Journal of Sedimentary Petrology, v. 61, p. 202–210.
Myrow, P.M., and Southard, J.B., 1996, Tempestite deposition: Journal of Sedimentary Research, v. 66, p. 875–887.
Myrow, P.M., Fischer, W., and Goodge, J.W., 2002, Wave-modified turbidites: combined-flow shoreline and shelf deposits, Cambrian, Central Transantarctic Mountains: Journal of Sedimentary Research, v. 72, p. 641–656.
Myrow, P.M., Hughes, N.C., Paulsen, T.S., Williams, I.S., Parcha, S.K., Thompson, K.R., Bowring, S.A., Peng, S.-C., and Ahluwalia, A.D., 2003, Integrated tectonostratigraphic reconstruction of the Himalaya and implications for its tectonic reconstruction: Earth and Planetary Science Letters, v. 212, p. 433–441.
Myrow, P.W., Thompson, K.R., Hughes, N.C., Paulsen, T.S., Sell, B.K., and Parcha, S.K., in press, Cambrian stratigraphy and depositional history of the northern Indian Himalaya, Spiti Valley, north-central India: Geological Society of America, Bulletin, v. 118.
Nanda, M.N., and Singh, M.P., 1976, Stratigraphy and sedimentation of the Zanskar area, Ladakh and adjoining parts of the Lahaul region of Himachal Pradesh: Himalayan Geology, v. 6, p. 365–388.
Parcha, S.K., 1998, Trace fossils from the Cambrian of Zanskar (Ladakh Himalaya) and their stratigraphic significance: Geological Society of India, Journal, v. 51, p. 635–645.
Penland, S., Boyd, R., and Suter, J.R., 1988, Transgressive depositional systems of the Mississippi delta plain: a model for barrier shoreline and shelf sand development: Journal of Sedimentary Petrology, v. 58, p. 932–949.
Reed, F.R.C., 1934, Cambrian and Ordovician fossils from Kashmir: Palaeontologia Indica, v. 21, no. 2, p. 1–38.
Sageman, B.B., Rich, J., Arthur, M., Birchfield, G.E., and Dean, W.E., 1997, Evidence for Milankovitch periodicities in Cenomanian–Turonian lithologic and geochemical cycles, Western Interior U.S.A.: Journal of Sedimentary Research, v. 67, p. 286–301.
Savrda, C.E., Bottjer, D.J., and Gorsline, D.S., 1984, Towards development of comprehensive euxinic biofacies model: evidence from Santa Monica, San Pedro, and Santa Barbara Basins, California Borderland: American Association of Petroleum Geologists, Bulletin, v. 68, p. 1179–1192.
Saxena, M.N., 1971, The crystalline axis of the Himalaya, Indian shield and continental drift: Tectonophysics, v. 12, p. 433–447.
Schlager, W., 1981, The paradox of drowned reefs and carbonate platforms: Geological Society of America Bulletin, v. 92, p. 197–211.
Schwartz, R.K., Cooper, D.W., and Etheridge, P.H., 1997, Sedimentologic architecture of the shoreface prism, relationship to profile dynamics, and relevance to engineering concerns: Duck, North Carolina: US Army Corps of Engineers, Technical Report CHL-97-19, Washington, D.C., 93 p.
Scotese, C.R., and McKerrow, W.S., 1990, Revised world maps and introduction: Palaeozoic Palaeogeography and Biogeography: Geological Society of London, Memoir 12, p. 1–21.
Searle, M.P., 1986, Structural evolution and sequence of thrusting in the High Himalayan, Tibetan–Tethys and Indus suture zones of Zanskar and Ladakh, Western Himalaya: Journal of Structural Geology, v. 8, p. 923–936.
Shah, S.K., Kumar, A., and Sudan, C.S., 1996, Agnostid trilobites from the Cambrian sequence of Zanskar and their stratigraphic significance: Current Science, v. 71, p. 951–954.
Srikantia, S.V., Ganesan, T.M., Rao, P.N., Sinha, P.K., and Tirkey, B., 1980, Geology of the Zanskar Area, Ladakh Himalaya: Himalayan Geology, v. 8, p. 1009–1033.
Vail, P.R., Mitchum, R.M, Jr., Todd, R.G., Widmier, J.M., Thompson, S.III, Sangree, J.B., Bubb, J.N., and Hatlelid, W.G., 1977, Seismic stratigraphy and global changes of sea level, *in* Payton, C.E., ed., Seismic Stratigraphy—Applications to Hydrocarbon Exploration: American Association of Petroleum Geologists Memoir #26, p. 49–212.
Van Wagoner, J.C., Ponsamentier, H.W., Mitchum, R.M., Vail, P.R., Sarg, J.F., Loutit, T.S., and Hardenbol, J., 1988, Overview of the fundamentals of sequence stratigraphy and key definitions, *in* Wilgus, C.K., Hastings, B.S., Kendal, C.G, St.C., Posamentier, H.W., Ross, C.A., and Van Wagoner, J.C., eds., Sea-Level Changes—An Integrated Approach: SEPM Special Publication No. 42, p. 39–45.
Walker, R.G., 1984, Shelf and Shallow marine sands, *in* Walker, R.G., ed., Facies Models, Second Edition: Geological Association of Canada, p. 141–170.
Whitaker, J.H.M., 1973, "Gutter Casts," a new name for scour-and-fill structures: with examples from the Llandoverian of Ringerike and Malmoya, southern Norway: Norsk Geologisk Tidsskrift, v. 53, p. 403–417.
White, W.A., 1961, Colloid phenomena in sedimentation of argillaceous rocks: Journal of Sedimentary Petrology, v. 31, p. 560–570.
Whittington, H.B., 1986, Late middle Cambrian trilobites from Zanskar, Ladakh, northern India: Rivista Italiana di Paleontologia e Stratigrafia, v. 92, p. 171–188.
Wignall, P.B., and Myers, K.J., 1988, Interpreting benthic oxygen levels in mudrocks: A new approach: Geology, v. 16, p. 452–455.
Yokokawa, M., 1995, Combined-flow ripples; genetic experiments and applications for geologic records: Kyushu University, Memoirs, Faculty of Science, Series D, Earth and Planetary Sciences, v. 29, p. 1–38.

Received 12 July 2004; accepted 6 July 2005.